筑　波　大　学

博 士 （医 学） 学 位 論 文

Right Ventricular Involvement and Outcome in Cardiac Sarcoidosis: Multimodality Imaging Findings

（心サルコイドーシスにおける右室病変と予後との関連：マルチモダリティイメージング解析による検討）

2022

筑波大学大学院博士課程人間総合科学研究科

Noor Kareem Khalaf Albakaa

参　考　論　文

心サルコイドーシス症例における右室長軸方向ストレインと心血管イベントとの関連

This thesis is based on the following original article **(Association between Right Ventricular Longitudinal Strain and Cardiovascular Events in Patients with Cardiac Sarcoidosis).** Noor K. Albakaa, MD, Kimi Sato, MD, PhD, Noriko Iida, RDCS, PhD, Masayoshi Yamamoto, MD, PhD, Tomoko Machino-Ohtsuka, MD, PhD, Tomoko Ishizu, MD, PhD, and Masaki Ieda, MD, PhD. **Published in Journal of Cardiology.** Doi.org/10.1016/j.jjcc.2022.07.015.

Table of Contents

4-List of Abbreviations

ACE, angiotensin-converting enzyme.

ACEI, angiotensin-converting enzyme inhibitor.

ARB, angiotensin II receptor blocker.

BNP, brain natriuretic peptide.

CS; cardiac sarcoidosis.

CMR, cardiac magnetic resonance imaging.

ECG, electrocardiogram.

FAC, fractional area change.

FDG-PET, 18F-fluorodeoxyglucose positron emission tomography.

GLS, global longitudinal strain.

IVS, interventricular septum.

JCS, Japanese circulation society.

LGE, late gadolinium enhancement.

LAVi, left atrial volume index.

LVEDVi, left ventricular end-diastolic volume index.

LVEF, left ventricular ejection fraction.

LV, left ventricular.

LVMi, left ventricular mass index.

LVESVi, left ventricular end-systolic volume index.

MR, mitral regurgitation.

NYHA, New York Heart Association.

RV, right ventricle.

RVD, right ventricular dysfunction.

RVFWLS, right ventricular free wall longitudinal strain.

sIL-2R, soluble interleukin-2 receptor.

SPECT, single-photon emission computed tomography.

S', tricuspid lateral annular systolic velocity on tissue Doppler imaging.

TAPSE, tricuspid annular plane systolic excursion.

TR, tricuspid regurgitation.

5- Background

5.1 Clinical Manifestations of Cardiac Sarcoidosis

Sarcoidosis is a multisystemic disease of unknown etiology that most commonly affects the lung, skin, heart, eye, and central nervous system. It is characterized by non-caseating epithelioid granulomatous infiltration. In Japan the sarcoidosis prevalence is 7.5 to 9.3 per 100,000 persons, and the yearly incidence is 1 per 100,000 persons [1]. Approximately 25% of patients with systemic sarcoidosis have cardiac involvement. Cardiac sarcoidosis (CS) is the leading cause of morbidity and mortality in sarcoidosis patients [1-3].

The manifestations of CS depend on the size and the location of the granulomatous infiltration. The presence of a small area of infiltration can be asymptomatic and only diagnosed by routine health checkups. At the same time, granulomatous infiltration to cardiac ventricles might cause thinning or aneurysm, which might lead to ventricular arrhythmias. One of the common sites for infiltration is the basal interventricular septum (IVS). Thinning of the basal part of the IVS is a specific sign of CS and is associated with the atrioventricular block (AVB) and a high risk of cardiac events [1-4]. CS can cause localized or generalized wall motion abnormality. While involved, a large area of left ventricle (LV) and right ventricle (RV) causes heart failure symptoms [1-3]. Valvular regurgitation is also observed in CS. It could be either due to the dilatation of the ventricle, which leads to valvular annulus dilatation, or direct infiltration of the papillary muscle [1,5]. Patients with CS may be presented with AVB, atrial or ventricular arrhythmia, or any ECG abnormality, which developed due to the infiltration of the conduction system or myocardium, or it can be due to the dilatation of the cardiac chamber [1-3]. In general, CS could be presented with different manifestations, which make its diagnosis difficult.

5.2 Diagnosis and treatment of cardiac sarcoidosis

Systemic sarcoidosis is the involvement of at least two organs (including the lymph node). Diagnosis of sarcoidosis is confirmed either by the presence of the non-caseating granulomatous infiltration or the presence of a specific finding in the affected organ. Patients with sarcoidosis should have periodic checking to determine early cardiac involvement [1,3].

Diagnosis of CS is challenging as it might mimic other cardiac conditions such as dilated cardiomyopathy, cardiac hypertrophy, chronic myocarditis, right arrhythmogenic cardiomyopathy, and ischemic heart disease [1-3]. The most specific test for CS diagnosis is an endomyocardial biopsy (EMB) (Figure 1); however, it has low sensitivity due to the patchy nature of the granulomatous infiltration [1,3].

The Japanese Circulation Society (JCS) guidelines for diagnosing and treating CS (2016) set clinical, imaging, and histological criteria to diagnose CS [1]. In JCS guidelines, the criteria for CS diagnosis are categorized into major criteria, which include (high-grade atrioventricular block, ventricular arrhythmias, thinning of the basal interventricular septum, left ventricular ejection fraction (LV EF) <50%, or regional wall motion abnormality, abnormal cardiac accumulation on Ga citrate scintigraphy of FDG-PET and late gadolinium enhancement (LGE) on CMR, and minor criteria which include abnormal ECG findings: ventricular arrhythmias (non-sustained VT, multifocal or frequent PVC), bundle branch block, axis deviation, or abnormal Q waves, perfusion defects on myocardial perfusion scintigraphy (SPECT), EMB with monocyte infiltration and moderate or severe myocardial interstitial fibrosis. To fulfill the CS diagnosis, two or more from the major or one from the major and two or more from the minor are required to diagnose CS with systemic sarcoidosis, while for isolated CS, at least four major criteria, including positive FDG uptake and one of the minor criteria [1].

Patients with active CS are treated with steroids as first-line therapy for inflammation suppression [1,6]; however, for intractable cases or when there is a contraindication for using steroids, other immune suppressive drugs (methotrexate, azathioprine, cyclophosphamide, etc.). Further treatment is required according to the patient's condition as heart failure, arrhythmias, and non-pharmacological treatment, which includes cardiac device implantation (pacemaker, intracardiac defibrillator, cardiac resynchronization therapy), catheter ablation, surgical treatment, and heart transplant [1].

5.3 Outcome of Cardiac Sarcoidosis

Historical series suggested a 5-year survival rate of 60% in patients with CS [7]. However, contemporary data showed 5-year survival as 96%, indicating the improvement of their survival with the appropriate use of anti-inflammatory medications, antiarrhythmic medication, and device implantation [8].

While the general outcome in CS has been improved, several prior data showed that severe LV dysfunction due to advanced sarcoidosis involvement in LV was associated with an increased risk of death or ventricular arrhythmia and poor recovery on LV systolic function by steroid therapy [1,7]. Other study also showed that RV involvement detected by CMR was independently associated with cardiac events, mainly ventricular arrhythmia [9]. Because the electrophysiological studies showed that the arrhythmogenic substrate in CS patients with ventricular tachycardia was mainly in RV [10], detecting RV involvement may provide additive information in detecting high risk patients in CS population.

Although, most of the CS patients have predominant LV disease and the extent of RV involvement was associated with the severity of LV involvement [11], it has been observed that up to 90% of the patients who had confirmed CS by either autopsy or by histological examination after the heart transplant had RV involvement [12], RV involvement was also observed by CMR [9,11,13,14]. Furthermore, few prior reports have highlighted the patients presented with RV predominant symptoms or isolated RV involvement [15]. Since there was a paucity of data if RV dysfunction sorely reflects the extent of LV damage by CS, detecting RV dysfunction in CS may help us to detect patients with predominant RV disease and higher risk of arrhythmic events.

Moreover, in recent decades there has been growing interest in studying the RV involvement and dysfunction in many cardiac diseases, especially with the advancement in imaging techniques. Accumulated evidence has shown the prognostic impact of the RV function on the outcome of cardiac diseases such as heart failure and valvular heart disease [16-18]. While limited data are available regarding the right ventricular (RV) involvement and function in CS [9,11,13-15,19], one study showed that low RV ejection fraction assessed by CMR and LGE in the RV wall was associated with a poor prognosis [9]; however, this study did not assess the FDG uptake in the RV wall and did not evaluate RV function by echocardiographic parameters. Despite the fact that the CMR is the golden tool to assess right ventricular function, there are many limitations to its use in many patients due to the contraindications to MRI or LGE evaluation (i.e., the existence of temporary pacemaker, lead abandonment due to cardiac implantable electronic device upgrade, the existence of non-MRI-conditional devices, allergy to gadolinium contrast medium, or chronic kidney disease) or limited access to CMR facilities that accept MRI-conditional devices. So, it is important to depend on the echocardiographic parameters to evaluate cardiac function status, especially during follow-up, as it is convenient and available.

5.4 Right Ventricular Functional Assessment by the Conventional Echocardiographic Parameters

Assessment of RV function by echocardiography is challenging due to its unique morphology (thin wall, triangular shape in the longitudinal axis and crescent shape in the short axis, heavy trabeculation) and location beneath the sternum [20,21].

Several parameters have been applied to overcome these limitations. The parameters that are recommended by the guidelines are the followings (Figure 2):

1- **Fractional area change (FAC)** by two-dimensional mode with (RV diastole area -

RV systole area / RV diastole area) × 100, the cutoff point is < 35%.

2- **Tricuspid annular plane systolic excretion (TAPSE)** on M-Mode. The cutoff of TAPSE is <17 mm.
3- **Tricuspid lateral annular systolic velocity (S')** on tissue Doppler imaging. The cutoff of the S' is <9.5 cm/s.

TAPSE and S' are angle-dependent parameters that measure the distance and velocity (respectively) of movement of the lateral tricuspid annulus between systole and diastole, this movement which sometimes affected by the severity of the tricuspid regurgitation (TR).

5.5 Right Ventricular Functional Assessment by the Right Ventricular Free Wall Strain (RVFWLS)

RVFWLS is a relatively novel parameter that measures the relative longitudinal shortening of the entire RV-free wall by 2D-spekcle tracking echocardiography.

2D-speckle tracking technique allow us to track the myocardium for multiple directions and describes the strain as deformation of an object normalized to its original shape and size [22]. As a hypothetical one-directional object can only change the length in one direction, strain can be calculated as the follows: Strain = [L(t)-L0]/L0, where L(t) is the length at a given point in time and L0 is the reference length at the reference time t0 and described as a percent [22]. Because reference time is usually taken at end-diastole and the length in systole is less than the length in diastole so the value of strain would be negative number if their myocardial function is normal. Therefore, larger absolute number of the strain means better longitudinal ventricular function, while lower absolute number of the strain means deteriorated ventricular function. Figures 3 shows the representative image of RVFWLS in patients with preserved and deteriorated RV function: patients with RVFWLS = -30%, the absolute number is 30 which indicated good RV function (Figure 3B), while a patient with RVFWLS = - 7.8 %, the absolute number is 7.8, indicating RV dysfunction (Figure 3C). Mean and lower limit of normal for RVFWLS have been reported as -26.9% (95%CI: -28.0, -25.9%) and -18.0% (95%CI: -19.2, -16.9%), respectively [23]

While RVFWLS is a relatively new parameter, several data showed its advantage over conventional RV parameters [16, 17]. As the RV stroke volume mainly depends on the RV wall longitudinal shortening during the systole [24,25], so RVFWLS is relatively a reflect of the actual RV function. Also, the RVFWLS is less angle dependent and less affected by LV dysfunction compared to the conventional parameters [16,20,21]. In addition to that, RVFWLS has shown a linear relationship with myocardial fibrosis in the patients with severe heart failure

who underwent heart transplant [26]. Furthermore, several studies have shown the prognostic impact of RVFWLS in cardiac diseases [16,17]. Therefore, I sought to evaluate the RV function in patients with CS using RVFWLS and its association with prognosis and reversibiltiy during steroid therapy. Also incorporating echocardiographic data with other imaginge modalities such as CMR and FDG-PET may help to understand if RV dysfunction in CS is solely the reflection of advanced stage of the disease or predominant RV disease.

6- Purpose

The purpose of this study is to investigate the following:

1- The association of the impaired RVFWLS and outcome in CS.
2- The association between impaired RVFWLS and CS involvement pattern in LV and RV.

The hypothesis of this thesis is that impaired RVFWLS is associated with poor outcomes in CS, and it could be an indicator of RV involvement in CS.

7-Method

7.1 Study Population

The study protocol was approved by the Ethical Review Committee of the University of Tsukuba Hospital (H30-325). Data were deidentified, and the requirement for informed consent was waived.

Figure 4 shows the patients selection. Fifty-one consecutive patients diagnosed with CS at the University of Tsukuba Hospital between 2012 and 2020 were retrospectively identified. CS was diagnosed according to the diagnostic criteria of the Japanese Circulation Society guidelines [1]. In brief, all patients underwent clinical evaluation, including a history of arrhythmic events, a 12-lead electrocardiogram (ECG), 2-dimensional (2D) and Doppler echocardiography, baseline blood test, FDG-PET, ^{67}Ga citrate scintigraphy, and gadolinium-enhanced CMR imaging. Histological diagnoses were made according to the confirmation of noncaseating epithelioid granulomas on endomyocardial biopsy. Clinical diagnoses were made in patients with extracardiac sarcoidosis when two or more of the five major criteria or one major criterion and two or more minor criteria were satisfied. In patients with no evidence of extracardiac involvement, isolated CS was diagnosed if at least four major criteria were satisfied, including abnormal accumulation of FDG-PET [1].

Demographic and clinical data at the time of diagnosis were obtained via manual extraction from the electronic medical records. The elevation of angiotensin-converting enzyme (ACE) and soluble interleukin-2 receptor (sIL-2R) levels was defined as ACE >29.4 IU/L and sIL-2R >613 U/ml. Patients were followed up via chart review using either the date of the last follow-up or the recorded date of death. The outcome data were last queried in August 2020. The primary outcomes were major adverse cardiovascular events (MACEs), including ventricular fibrillation, sustained ventricular tachycardia (VT), advanced heart block, and heart failure hospitalization.

7.2 Conventional Echocardiographic Parameters

All patients underwent comprehensive echocardiographic assessments using commercially available ultrasound systems; all measurements were performed at the baseline and 1 year after steroid therapy according to the current guidelines [20,21,27]. Echocardiographic variables included LV ejection fraction (LVEF), LV end-diastolic volume (LVEDV), LV end-systolic volume (LVESV), left atrial volume index, mitral LV inflow peak early (E) and late diastolic (A) velocities, peak early diastolic velocity of the septal and lateral mitral annulus (e’), and

peak tricuspid regurgitation (TR) velocity. LVEF, LVEDV, and LVESV were calculated using the biplane method of discs. The probability of pulmonary hypertension (PH) was assessed according to the guideline [28].

RV function parameters included tricuspid annular plane systolic excretion (TAPSE), fractional area change (FAC), and tricuspid lateral annular systolic velocity on tissue Doppler imaging (S') [20]. All RV function parameters were retrospectively evaluated by experienced echocardiographers who were blinded to the clinical information. Abnormal cut-offs for RV function parameters were as follows: TAPSE <17 mm, S' <9.5 cm/s, and FAC <35% [20]. RV function was considered abnormal if >50% of the available RV function parameters were abnormal [18].

7.3 Two-Dimensional Strain Analysis

2D strain analysis was assessed offline using commercially available, vendor-independent software (Image Arena 4.6; TOMTEC Imaging Systems GmbH, Munich, Germany). To get the RVFWLS it is required to have a good image quality with clear endocardial border of the RV, then to select three points of the RV endocardial wall (first point at the base of the lateral tricuspid annulus, second point at the RV basal septum and the last point is in the RV apex). After tracing the endocardial border on the end-systolic frame, the software automatically tracked the contour and performed speckle tracking on the subsequent frames. RVFWLS was estimated by the average longitudinal strain in the free wall segment in the RV focused apical four-chamber view (Figure 5A).

LV global longitudinal strain (LVGLS) was estimated using the average peak systolic longitudinal strain from the apical four-chamber, two-chamber, and long-axis views.

All strain measurements were performed by a single observer who remained blinded to the clinical and echocardiographic data, as well as the outcomes. To assess the intra- and interobserver variability of the strain measurements, 10 datasets were randomly selected; two observers analyzed the same datasets on two different occasions—separated by a 1-week interval—without knowledge of the other observer's measurements. The intraclass correlation coefficient showed the intraobserver variability of RVFWLS was 97%, whereas the interobserver variability was 90%. Percent variability of intraobserver and interobserver variability was 3.8% and 4.8%, respectively.

7.4 FDG-PET Imaging Analysis

FDG-PET imaging was used to detect myocardial inflammation associated with active CS involvement. All patients underwent dietary preparation 24 h prior to PET scanning. A high-fat diet was followed, and carbohydrates, sugars, dairy, and starchy foods were avoided; this was followed by a prolonged fast for 18 h to suppress physiological myocardial FDG uptake. FDG-PET imaging was performed according to guidelines [1,29].

PET images were qualitatively analyzed, and LV myocardial FDG uptake was visually categorized into four patterns: none, diffuse, focal, and focal on diffuse. Focal and focal on diffuse were recognized as positive scans [1,29]. The presence of focal uptake within the RV-free wall was also evaluated (Figure 5B). The FDG accumulation for the LV myocardial segment was assessed using the American Heart Association 17-segment model [27]. For analysis, we simplified the LV segmentation (Figure 6). For septal segments, anteroseptal and inferoseptal segments in basal and mid were considered the same segment. As for remaining anterior, anterolateral, inferolateral, and inferior segments, basal and mid segments were merged and considered as the same segment. Four apical segments and an apex were exhibited as one segment. Distribution of FDG-uptake in RV was evaluated for RV free-wall only due to the spatial resolution.

7.5 Cardiac Magnetic Resonance Imaging Analysis

LGE was evaluated to detect the myocardial scar related to the CS using CMR. CMR was performed using a 1.5 T scanner according to a standardized protocol. Cine imaging was acquired with a steady-state free precession breath-hold sequence in contiguous slices. Imaging with LGE as acquired after 10-15 minutes after intravenous gadolinium injection. Quantitative analysis of LGE was performed on short-axis LGE sequences, and normal septal myocardium was selected as a reference region, and the signal > 6 SD above normal myocardium was quantified by using commercially available software (CMR42, Circle Cardiovascular Imaging Inc., Calgary, Canada). LGE was identified visually in LV and RV (Figure 5C). The distribution of LGE in LV was analyzed using the same segmentation used for the FDG-PET. The endocardial RV surface was divided into RV-free wall and septum.

7.6 Electrophysiological Evaluation During Catheter Ablation

In patients who underwent catheter ablation of VT, the distribution of bipolar low voltage area within the LV and RV was evaluated. The bipolar low voltage area was defined as an area within 0.5-1.5 mV. Ablation was done either during VT in hemodynamically stable patients or

during sinus rhythm based on substrate mapping (like voltage map or pace map) when the patients were hemodynamically unstable, or the VT was non inducible.

7.7 Statistical Analysis

Continuous variables were presented as mean ± standard deviation when normally distributed or median (interquartile range [IQR]) if non-normally distributed. Categorical variables were presented as numbers and percentages. Clinical and echocardiographic parameters between the two groups were compared using the unpaired t-test, Mann-Whitney test, or chi-square test, while echocardiographic parameters before and after medical therapy were compared using the paired t-test or Wilcoxon signed-rank test, as appropriate. Cox proportional hazards analysis was performed to assess the association between echocardiographic variables and outcomes. In a multivariable model, all relevant variables and possible confounding factors, which were selected because of their known prognostic value, were entered into the model using stepwise selection. We also estimated the propensity score for reduced RVFWLS (> -16.8%) using the multivariable logistic regression model with known predictors of CS (age, sex, prior atrioventricular block [AVB], sustained VT, LVEF, LGE, and FDG-PET accumulation) .The propensity score was entered into the multivariable model as a covariate to reduce the imbalance in baseline variables. Receiver operating characteristic curve analysis was also performed to determine the diagnostic value of RVFWLS for detecting MACE. Receiver operating characteristic curve analysis was also performed to determine the diagnostic value of RVFWLS for detecting MACE. Event-free survival was analyzed using Kaplan-Meier survival analysis, and the survival across groups was compared using the log-rank test. Logistic regression models with continuous net reclassification improvement (NRI) were used to assess the incremental predictive performance of RVFWLS [30]. To assess differences in changes in echocardiographic parameters between groups over time, we used a linear mixed effects model with unstructured covariance. The model was constructed using patient groups and time as covariates. The slope of regression line obtained using a mixed model is presented along with the corresponding box plots of the actual measurements to show change of parameters over time. A two-sided p-value <0.05 was considered statistically significant, and all statistical analyses were performed using SPSS (version 26.0; SPSS Inc., Chicago, IL, USA) and R software version 3.2.2 (R Foundation for Statistical Computing, Vienna, Austria).

8- Result

8.1 Patient Characteristics

A total of 51 patients with CS who underwent steroid therapy were identified (Figure 7). In addition to prednisone, eight patients received other immunosuppressants (methotrexate, 7; azathioprine, 1) due to the lack of response to prednisone alone. At the time of diagnosis, 19 patients (37%) had implanted cardiac device (11 patients had pacemaker, 5 patients had implantable cardioverter defibrillator [ICD] and 3 patients had cardiac resynchronization therapy [CRTD]). Furthermore, in the entire cohort, 51% had beta blocker, 53% had either angiotensin-converting enzyme inhibitor or angiotensin-converting enzyme blocker, and 55% were on amiodarone at baseline. The mean age of the patients was 63±11 years and 33 (61%) were female. Details regarding the patients' baseline characteristics are shown in Table 1. Thirty-two patients (63%) exhibited clinical evidence of extracardiac involvement; the remaining 19 patients did not display any extracardiac involvement and were diagnosed with isolated CS. Four patients (8%) were histologically diagnosed with CS. The prevalence of major and minor criteria for cardiac involvement in the study population are described in Table 2. Among the 30 patients who had arrhythmic events at presentation, 20 patients had high-grade atrioventricular block, 15 had sustained VT, and 2 had ventricular fibrillation. Out of the 15 patients who presented with VT, 12 of them received radiofrequency catheter ablation or introduction of antiarrhythmic medications, Additionally, FDG-PET and CMR evaluation were available in 51 (100%) and 34 (67%) patients at the baseline, respectively.

Table 3 shows the baseline echocardiographic parameters. The mean LVEF was 50±14%, and 25 patients (49%) had an LVEF <50%. Among the study population, none of them showed the echocardiographic findings suggesting PH. Moreover, among the 31 patients who underwent right heart catheterization, 8 patients showed PH and all of them had elevated pulmonary capillary wedge pressure indicating post-capillary PH. According to the conventional RV function parameters, RVD was observed in nine patients (18%). The mean RVFWLS was -19.1±5.2% (median -18.0%; IQR -22.5 to -15.0%).

8.2 Clinical Outcome

All patients underwent steroid therapy after the diagnosis of CS. The mean initial dose of steroid was 31±3 mg and was tapered to 7±3 mg. Except one patient all patients received less than equal 10 mg of steroid as maintenance dose (5mg or less: 48%, more than 5 to 10mg: 50%). Steroid sparing agents were newly added for eight patients (seven had methotrexate and

one had azathioprine) at a median period of 544 (IQR 504-729) days after index visit due to the recurrence of the disease. Also 18 patients (36%) had implanted cardiac device during follow-up (pacemaker, 6; ICD, 5; CRT-D, 7) (Table 4). During the median follow-up period of 549 (IQR 350–949) days, 11 (22%) patients exhibited MACEs, 6 patients had sustained VT, 1 patient had ventricular fibrillation, 3 were hospitalized for decompensated heart failure, and 1 developed atrioventricular block requiring pacemaker implantation. None of our patients developed other cardiac events such as stroke or myocardial infarction. Among the six patients who developed sustained VT, four of them experienced recurrence (recurrence rate, 31%). None of the patients underwent heart transplantation or died due to CS.

When the patients' characteristics were compared according to the outcome, patients experienced events trended toward a higher prevalence of arrhythmic events (9 [89%] vs. 21 [53%], P = 0.08) and lower prevalence of FDG-PET abnormality (10 [91%] vs. 40 [100%], P= 0.054; Table 2). Patients with events also showed worse RVFWLS than event-free patients (-15.7 ±4 vs - 20.1 ± 5.1, p = 0.013; Table 3). Notably, when we further compared the RVFWLS value according to the type of event, the patients who developed sustained VT showed lower RVFWLS than those without VT (-15.2±2.9% vs. -19.8±5.2%, P = 0.013). Patients who had heart failure hospitalization also showed a trend toward lower RVFWLS than those without heart failure events (-14.8±1.5% vs. -19.4±5.2%, P= 0.068). Patients with events showed a trend toward higher prevalence of basal IVS thinning than others (7 [64 %] vs 14 [35 %], P = 0.09), while other conventional RV function parameters and LV function parameters were similar in both groups.

In the univariable Cox proportional hazards model analysis, RVFWLS was found to be associated with MACEs (hazard ratio [HR]: 1.29, 95% CI: 1.07–1.57; P=0.008; Table 5). Sustained VT at baseline (HR: 5.26, 95%CI: 1.54-18.05; P = 0.008) was also associated with MACEs. In the multivariable model, all possible confounding factors were added such as age, sex, prior AVB, sustained VT, and LVEF, using forward stepwise selection. The multivariable model revealed that RVFWLS (HR: 1.22, 95% CI: 1.03–1.46; P=0.025) and prior sustained VT (HR: 4.20, 95% CI: 1.16–15.17; P=0.028) were independently associated with MACEs. Furthermore, since I only have small number of patients who developed outcome, I constructed propensity score for RVFWLS by using known characteristics to eliminate potential bias. Propensity scores were entered into the multivariable model as a covariate. After adjusting for the propensity score, deteriorated RVFWLS was still associated with higher incidence of MACEs (HR: 1.22, 95%CI: 1.004-1.48; P = 0.045).

In other to illustrate the outcome according to the RVFWLS value, I subdivided patients into three groups according to the RVFWLS tertiles: tertile 1 (RVFWLS < -21.0%, most preserved RVFWLS group, n = 17), tertile 2 (RVFWLS -12.0 to 16.8%, n = 17), tertile 3 (RVFWLS >-16.8%, most deteriorated RVFWLS group, n =17). Kaplan-Meier curves of the study population, stratified according to the RVFWLS tertiles, revealed that patients with more deteriorated RVFWLS (>-16.8%, 3rd tertile) were associated with poorer event-free survival than other groups (P=0.002; Figure 8).

Compared with conventional parameters, RVFWLS demonstrated the highest area under the curve (RVFWLS: 0.74, TAPSE: 0.54, S': 0.60, FAC: 0.48; Figure 9). The optimal cut-off value for RVFWLS allowing for the prediction of MACEs was >-16.8%, demonstrating a sensitivity and specificity of 82% and 77%, respectively. RVFWLS also showed a significant incremental value over RVD defined according to conventional parameters with NRI of 0.71 (95% CI: 0.09–1.33; P=0.02).

8.3 Changes in RV Parameters during Steroid Therapy

Table 6 shows echocardiographic parameters at the baseline and 1 year after steroid therapy. One year after steroid therapy, patients with events demonstrated trends toward TAPSE, RVFWLS, and LVGLS deterioration. On the contrary, event-free patients showed similar RV function parameters over time and significant improvement in LVGLS (-10.5± 2.8% vs. -14.5 ±4.3%, P= 0.014). The magnitude of changes in echocardiographic parameters between the patients with events and those without events was compared using a mixed-effects model; patients with events demonstrated a trend toward worsening RVFWLS at 1 year after steroid therapy compared with patients without events (+2.7% after 1 year; P=0.11; Fig. 7A). Patients with events at the baseline also demonstrated deteriorating TAPSE (-2.7% after 1 year; P=0.14; Fig. 7B). LVGLS was also significantly deteriorated in patients with events (+3.6% after 1 year; P= 0.03; Fig. 7E) than those without events.

8.4 Imaging Characteristics of Patients with RV Dysfunction

When comparing the baseline echocardiographic characteristics between patients with or without RVD according to the RVFWLS, patients with RVD showed higher BNP levels (223 [109- 437] pg/ml vs. 113 [51 -201] pg/ml, P = 0.032), lower LVEF (42.4 ± 11.9% vs. 53.4 ± 13.3%, P=0.005), and LVGLS (-10.4± 3.9% vs. -13.3±4.6%, P= 0.049) compared with those without RVD (Table 7). Of the 51 patients, 50 had FDG-PET images available for evaluation

of abnormal accumulation in the RV wall. Abnormal FDG accumulation was observed in 19 patients (38%); of these, 14 (74%) exhibited a focal uptake pattern, while the remaining 5 patients (26%) exhibited a diffuse pattern. Patients with reduced RVFWLS (> -16.8%) showed trend toward higher prevalence of RV uptake compared with those with preserved RVFWLS [10 (56%) vs. 9 (28%), P = 0.06). Among the 34 patients with CMR evaluation, 15 (44%) patients had LGE in the RV wall. Patients with reduced RVFWLS showed a higher prevalence of RV LGE compared with those with preserved RVFWLS [8 (73%) vs. 7 (30%), P= 0.02].

To investigate the association of RV involvement detected CMR and FDG-PET with LV and RV echocardiographic parameters, the patients were divided into two groups according to their existence of FDG accumulation and LGE in RV. As shown in Table 8, patients with FDG uptake in RV showed lower RV FAC and RVFWLS, indicating the existence of RV dysfunction. While LV function parameters were similar in both groups. Similarly, patients with LGE in RV free wall showed significant deterioration in FAC and RVFWLS (Table 9), while there were no significant differences regarding their LV EF and LV GLS.

8.5 FDG-PET and CMR Findings in Patients with Impaired RVFWLS

Sub-analysis for 33 patients was performed with all imaging modalities (echocardiography, CMR, and PET) to evaluate the imaging characteristics in patients with deteriorated RVFWLS. The patients were divided into two groups according to their baseline RVFWLS to investigate the detailed distribution of LGE and FDG accumulation in each group (Table 10, Figure 11 and 12). Thirteen patients (39%) with reduced RVFWLS (RVFWLS >-16.8%) had significantly higher prevalence of LGE in the RV free wall (83% vs. 25%, p = 0.001) and RV septum (85% vs. 50%, P=0.043) compared to the patients with preserved RVFWLS. Of note, while we also compared the amount of LGE mass in LV, there was no difference in the total amount of the LGE between the two groups (31 ± 16 g vs. 26 ± 25 g, P=0.558). Reduced RVFWLS group also showed trend towards higher prevalence of RV free wall FDG accumulation than preserved RVFWLS group (62% vs. 35%, p = 0.135). At the same time, the distribution of the LGE and the FDG accumulation in LV segments did not show any significant difference, suggesting that patients with RV dysfunction detected by RVFWLS>-16.8% may have more predominant RV disease (Figure 11 and 12).

8.6 Electrophysiological Evaluation During Catheter Ablation

Seven patients underwent catheter ablation of VT. Table 11 showed the electrophysiological findings and ablation site during catheter ablation of VT. Among seven patients who underwent catheter ablation of VT, two of them had normal voltage map in LV and RV. Remaining five patients had low voltage area in the RV. Ablation site involved RV in five patients.

9- Discussion

In this study, RVFWLS demonstrated additive value as a surrogate for RVD over conventional echocardiographic parameters, allowing us to detect CS patients with a higher risk of MACEs. Additionally, it may represent the best echocardiographic parameter required to evaluate RV function and outcomes in patients with CS during steroid therapy. Furthermore, deterioration of RV systolic function was associated with FDG-PET accumulation and LGE in the RV wall, suggesting that the RVFWLS can be utilized to evaluate CS activity and disease burden.

9.1 Clinical Implication of RVFWLS in Cardiac Sarcoidosis

While several prior studies have reported an association between RVD and outcomes in patients with CS, RV systolic function was only evaluated by CMR, using RVEF or the presence of LGE on the RV wall [9,11,13,14]. In the present study, RV function was evaluated, and the extension of cardiac involvement through comprehensive echocardiographic evaluation confirmed for the first time that RVFWLS was associated with poor outcomes in the CS population. Due to the complex nature of RV anatomy and physiology, CMR has been considered the gold standard tool for RV function assessment. Our study demonstrated that the echocardiographic evaluation of RV systolic function could play a crucial role in the risk stratification of patients with CS, as it is more feasible in daily practice and in places where CMR may not be readily available for evaluation. Furthermore, the RV strain measurement is easily to applied and is not time-consuming.

Additionally, the incremental value of RVFWLS was elucidated over conventional RVD parameters, such as TAPSE, S', and FAC. While TAPSE, S', and FAC are quantitative parameters recommended by the guidelines, their accuracy may be affected by the imaging plane, angle of the images, or regional abnormalities and tethering of the RV free wall [20]. RVFWLS is a relatively new echocardiographic technique that may overcome most of the limitations of conventional parameters, as it permits global assessment of the RV-free wall throughout the entire cardiac cycle [20]. Moreover, although the RVFWLS only incorporates one-motion direction, approximately 80% of RV stroke volume is driven by longitudinal changes in the RV free wall [24]; thus, it has established diagnostic and prognostic value regarding RV pathologies and additive value over TAPSE, S', and FAC in various cardiac diseases [16,17]. Prior data suggest the reliability of RVFWLS in detecting RVD; thus, this study demonstrates the clinical importance of RVFWLS in the risk stratification of individuals with CS as a reliable marker of RV function.

9.2 Right Ventricular Dysfunction in Cardiac Sarcoidosis

In the present study, patients with reduced RVFWLS exhibited a higher prevalence of FDG uptake in the RV-free wall and more advanced LV dysfunction, suggesting that active RV involvement is associated with RVD and poorer outcomes in patients with CS. In addition to the direct granulomatous infiltration of the RV wall, one can suspect that PH secondary to LV dysfunction, or lung involvement of sarcoidosis, could be the possible underlying mechanism of RVD [9,11,25,31]. In the present study, patients with RVD showed more advanced LV dysfunction and RV LGE on CMR when compared with the no RVD group, but none of them showed significant PH. This indicated that RVD detected based on RVFWLS was mainly associated with the extent of CS involvement rather than secondary PH. These data suggest that the RVFWLS is superior to detect the advanced stage of CS with a direct extent of RV involvement and advanced LV involvement.

Prior data suggested that most of the CS patients have predominant LV disease, hence the extent of RV involvement usually associated with severity of LV involvement [11,14]. However, I found that the quantitative LGE and its distribution in LV was not significantly different between the patients with reduced RVFWLS and those with preserved RVFWLS. This data suggested that those patients with reduced RVFWLS may have CS involvement more oriented to the RV, which might explain their higher event rate, especially arrhythmic events.

9.3 The Impact of Left Ventricular Involvement on Outcome

In this study, the LV echocardiographic parameters did not show an association with outcome compared with the prior studies that revealed an association between LV dysfunction and the outcome [32,33]. In one report, LV GLS was significantly associated with the outcome. It also highly predicated detection of LV LGE when preserved LVEF were included [32]. Another group showed that LVEF was independent predictor of MACE and the patients with LVEF < 50 % associated with worse outcome [33]. And those with LV EF < 35 % were more likely to have heart transplant [33]. In the current study, LVEF and GLS did not show significant difference between the patients with the event and those without. The discrepancy between the present data and the prior studies, could be explained by the differences in the inclusion criteria, the defined outcome, the small cohort sample, and fewer event rate.

In this study, I defined the primary outcome only including the event associated with CS such as ventricular fibrillation, sustained VT, AVB, and heart failure hospitalization. While the general cardiovascular events (stroke, myocardial infarction) had not included, none of the patients experienced those events. At the same time, the study population consist of the higher

prevalence of previous history of ventricular arrhythmia, inclusion of ventricular arrhythmia as primary endpoint may lead the bias due to their treatment for arrythmia. In patients with newly diagnosed CS, ventricular arrhythmias are commonly observed and are associated with advanced cardiac remodeling. On the other hand, several reports have shown that CS patients may suddenly develop VT and sudden cardiac death, regardless of the cardiac function [1,2]. Therefore, incorporating VT as the primary outcome is essential for describing the predictive utility of RVFWLS and understanding CS's clinical course. Furthermore, the multivariable analysis showed that RVFWLS (HR 1.22, 95%CI:1.03–1.46, p =0.025) was independently associated with the outcome independent of the baseline VT (HR 4.20, 95%CI:1.16–15.17, p = 0.028), indicating that RVFWLS could be an independent marker to predict cardiovascular events in patients with CS regardless of their presentation.

Moreover, in the present study, among 30 patients who had arrhythmic events at presentation, the majority had an advanced atrioventricular block. Also, all patients, except one, who presented with VT at the time of diagnosis, received radiofrequency catheter ablation or antiarrhythmic medications, which led to the suppression of VT in nine patients (69%) during follow-up. In CS, VA might be due to scar-related reentrant tachycardia, which occurs due to conduction disturbance created by the surviving myocytes in the vicinity of the scar tissue or area of active inflammation. Another cause is Purkinje network-mediated VA, such as Purkinje-related PVCs triggering VF or bundle branch reentrant VT [1]. Hence, the ablation outcomes depend on the extent of scarring or disease activity. Kumar et al. reported that a single ablation procedure successfully suppressed VT entirely in approximately 40% of patients and terminated VT storms that were not responding to pharmacotherapy in 71% of patients [10]. Current results align with previous reports and indicate that VT recurred in certain patients. Therefore, RVD detected by RVFWLS might be able to serve as clinical manifestations associated with the recurrence of VT and a higher risk of sudden cardiac death to indicate the requirement of a defibrillator.

9.4 Limitations

The present study had several limitations. First, this was a retrospective, observational study with a small population conducted at a tertiary referral center. However, this cohort represents the largest collection of CS patients who underwent comprehensive detailed RV function parameter evaluation by echocardiography. Second, the application of speckle tracking techniques depended on 2D image quality, which was suboptimal in some patients, thus, preventing reliable measurement. Furthermore, the control group was not included in this study

for RVFWLS evaluation. Nonetheless, a recent meta-analysis reported pooled mean and lower limit of normal for RVFWLS were -26.9% (95%CI: -28.0, -25.9%) and -18.0% (95%CI: -19.2, -16.9%), indicating RVFWLS > -16.9% would be considered abnormal [23]. This threshold was similar to the optimal cut-off value of RVFWLS > -16.8% developed in the present study and suggests the applicability of RVFWLS evaluation in the CS population. Additionally, while the association between RVFWLS and prognosis suggested that the underlying myocardial infiltration of granulomatous tissue affected outcomes, there was a lack of quantitative measures for myocardial damage in the present study. There was a potential risk of overfitting in the multivariable analysis as the number of events was low. Also, in this study LV parameters did not show significant association with end point, this might be related to the small cohort sample and limited event rate. The correlation between the LGE distribution in LV and it impact on the RV function could not be assessed in all patients as some patients did not have CMR study. Moreover, due to the retrospective nature of the study, therapeutic decisions were made by the physicians who were aware of all clinical information. This might affect the decisions for additional treatment, especially for arrhythmia and heart failure and may cause the hidden impact on our results. Furthermore, although RVFWLS showed serial changes during medical therapy and could serve as a marker during steroid therapy, it is not a direct measure of active inflammatory lesions nor an alternative diagnostic tool. Hence, prospective studies with a larger population incorporating CMR information with echocardiography and FDG-PET findings are required to confirm the pathophysiological mechanism and generalizability of the present results.

10- Conclusion

RVFWLS could be an independent predictor of MACEs in CS and may reflect the disease activity and extent in RV. This result highlights the importance of risk stratification using RVFWLS in patients with CS.

11- Summary figure

Right ventricular free wall longitudinal strain (RVFWLS)

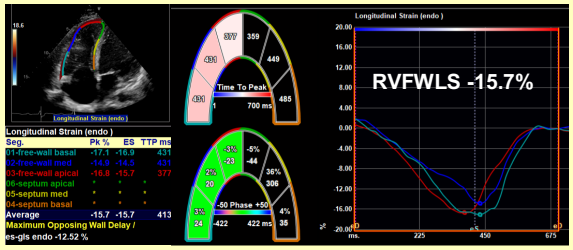

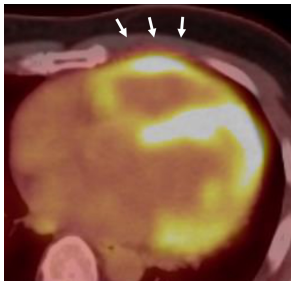

FDG uptake in RV free wall

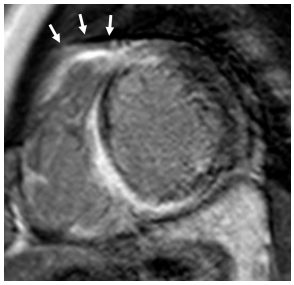

LGE in the RV free wall

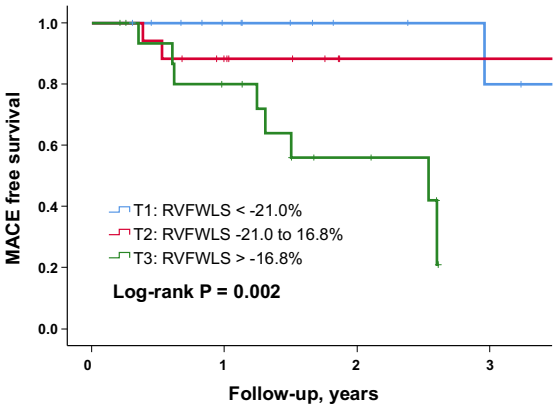

Impaired RVFWLS was associated with:
1- MACE.
2- RV free wall FDG uptake.
3- RV free wall LGE.

12- REFERENCES

1. Terasaki F, Azuma A, Anzai T, Ishizaka N, Ishida Y, Isobe M, et al. JCS 2016 Guideline on diagnosis and treatment of cardiac sarcoidosis - Digest version. Circ J 2019;83:2329-88.

2. Birnie DH, Nery PB, Ha AC, Beanlands RS. Cardiac sarcoidosis. J Am Coll Cardiol 2016;68:411-21.

3. Writing group; Document reading group; EACVI Reviewers: This document was reviewed by members of the EACVI Scientific Documents Committee for 2014–2016 and 2016–2018. A joint procedural position statement on imaging in cardiac sarcoidosis: from the Cardiovascular and Inflammation & Infection Committees of the European Association of Nuclear Medicine, the European Association of Cardiovascular Imaging, and the American Society of Nuclear Cardiology. Eur Heart J Cardiovasc Imaging 2017;18:1073-89.

4-Nagano N, Nagai T, Sugano Y, Morita Y, Asumi Y, et al. Association between basal interventricular septum and adverse longterm clinical outcomes in patients with cardiac sarcoidosis.Circ J 2015;79:1601-1608.

5-Roberts WC, MC Allister HAJr, FerransVJ. Sarcoidosis of the heart. A clinicopathological study of 35 necropsy patients (group I) and review of 78 previously described necropsy patients (group II). Am J Med 1977;63:86-108.

6. Chiu CZ, Nakatani S, Zhang G, Tachibana T, Ohmori F, Yamagishi M, et al. Prevention of left ventricular remodeling by long-term corticosteroid therapy in patients with cardiac sarcoidosis. Am J Cardiol 2005;95:143-6.

7. Yazaki Y, Isobe M, Hiroe M, Morimoto SI, Hiramitsu S, Nakano T, Izumi T, Sekiguchi M, et. al. Central Japan Heart Study Group. Prognostic determinants of long-term survival in Japanese patients with cardiac sarcoidosis treated with prednisone. The American journal of cardiology. 2001;88(9):1006-10.

8. Ribeiro Neto ML, Jellis CL, Joyce E, Callahan TD, Hachamovitch R, Culver DA, et.al. Update in cardiac sarcoidosis. Annals of the American Thoracic Society. 2019;1341-50.

9. Kagioka Y, Yasuda M, Okune M, Kakehi K, Kawamura T, Kobuke K, et al. Right ventricular involvement is an important prognostic factor and risk stratification tool in suspected cardiac sarcoidosis: analysis by cardiac magnetic resonance imaging. Clin Res Cardiol 2020;109:988-98.

10.Kumar S, Barbhaiya C, Nagashima K, Choi EK, Epstein LM, John RM, et. al. Ventricular tachycardia in cardiac sarcoidosis: characterization of ventricular substrate and outcomes of catheter ablation. Circulation: Arrhythmia and Electrophysiology. 2015 :87-93.

11. Smedema JP, van Geuns RJ, Ainslie G, Ector J, Heidbuchel H, Crijns H, et.al. Right ventricular involvement in cardiac sarcoidosis demonstrated with cardiac magnetic resonance. ESC Heart Fail 2017;4:535-44.

12- Okasha O, Kazmiczak, Amey Chen K,Frazneh-Far A,Shenoy C, etal..Myocardial involvment in patients with histologically diagnosed cardiac sarcoidosis: A systemic review and meta -analysis of gross pathological images from autopsy or cardiac transplantation cases. J Am Hear Assoc.2019;8:e011253.

13.Velangi PS, Chen KA, Kazmirczak F, Okasha O, von Wald L, Roukoz H, et al. Right ventricular abnormalities on cardiovascular magnetic resonance imaging in patients with sarcoidosis. JACC Cardiovasc Imaging 2020;13:1395-405.

14. Crawford T, Mueller G, Sarsam S, Prasitdumrong H, Chaiyen N, Gu X, et al. Magnetic resonance imaging for identifying patients with cardiac sarcoidosis and preserved or mildly reduced left ventricular function at risk of ventricular arrhythmias. Circ Arrhythm Electrophysiol 2014;7:1109-15.

15. Vakil, Kairav, Elina Minami, and Daniel P. Fishbein. "Right ventricular sarcoidosis: is it time for updated diagnostic criteria?" *Texas Heart Institute Journal* 41, no. 2 (2014): 203-207.

16. Carluccio E, Biagioli P, Lauciello R, Zuchi C, Mengoni A, Bardelli G, et al. Superior prognostic value of right ventricular free wall compared to global longitudinal strain in patients with heart failure. J Am Soc Echocardiogr 2019;32:836-44.e1.

17. Hamada- prognostic value of right ventricular strain in patients with acute decompensated heart failure. Circ Cardiovasc Imaging 2018;11:e007249.Harimura Y, Seo Y, Ishizu T, Nishi I, Machino-Ohtsuka T, Yamamoto M, et al. Incremental

18. Asami M, Stortecky S, Praz F, Lanz J, Räber L, Franzone A, et al. Prognostic value of right ventricular dysfunction on clinical outcomes after transcatheter aortic valve replacement. JACC Cardiovasc Imaging 2019;12:577-87.

19. Kusunose K, Fujiwara M, Yamada H, Nishio S, Saijo Y, Yamada N, et al. Deterioration of biventricular strain is an early marker of cardiac involvement in confirmed sarcoidosis. Eur Heart J Cardiovasc Imaging 2020;21:796-804.

20. Rudski LG, Lai WW, Afilalo J, Hua L, Handschumacher MD, Chandrasekaran K, et al. Guidelines for the echocardiographic assessment of the right heart in adults: a report from the American Society of Echocardiography endorsed by the European Association of

Echocardiography, a registered branch of the European Society of Cardiology, and the Canadian Society of Echocardiography. J Am Soc Echocardiogr 2010;23:685-713.
21. Badano LP, Kolias TJ, Muraru D, Abraham TP, Aurigemma G, Edvardsen T, et al. Standardization of left atrial, right ventricular, and right atrial deformation imaging using two-dimensional speckle tracking echocardiography: a consensus document of the EACVI/ASE/Industry Task Force to standardize deformation imaging. Eur Heart J Cardiovasc Imaging 2018;19:591-600.
22. Edvardsen, T., Donal, E., Bucciarelli-Ducci, C. and Maurovich-Horvat, P., Maurer, G., & Popescu, BA (2017). The years 2015-2016 in the European Heart Journal-Cardiovascular Imaging. Part I. European Heart Journal-Cardiovascular Imaging, 18 (10), 1092-1098.[jex192].
23 Wang TKM, Grimm RA, Rodriguez LL, Collier P, Griffin BP, Popović ZB. Defining the reference range for right ventricular systolic strain by echocardiography in healthy subjects: A meta-analysis. PLoS One 2021;16:e0256547.

24. Buckberg G, Hoffman JI. Right ventricular architecture responsible for mechanical performance: unifying role of ventricular septum. J Thorac Cardiovasc Surg 2014;148:3166-71.e1-4.
25. Haddad F, Doyle R, Murphy DJ, Hunt SA. Right ventricular function in cardiovascular disease, part II: pathophysiology, clinical importance, and management of right ventricular failure. Circulation 2008;117:1717-31.
26. Lisi M, Cameli M, Righini FM, Malandrino A, Tacchini D, Focardi M, et.al. RV longitudinal deformation correlates with myocardial fibrosis in patients with end-stage heart failure. JACC: Cardiovascular Imaging. 2015;514-22.
27. Lang RM, Badano LP, Mor-Avi V, Afilalo J, Armstrong A, Ernande L, et al. Recommendations for cardiac chamber quantification by echocardiography in adults: an update from the American Society of Echocardiography and the European Association of Cardiovascular Imaging. Eur Heart J Cardiovasc Imaging 2015;16:233-70.
28. Galiè N, Humbert M, Vachiery JL, Gibbs S, Lang I, Torbicki A, et al. 2015 ESC/ERS Guidelines for the diagnosis and treatment of pulmonary hypertension: The Joint Task Force for the Diagnosis and Treatment of Pulmonary Hypertension of the European Society of Cardiology (ESC) and the European Respiratory Society (ERS): Endorsed by: Association for European Paediatric and Congenital Cardiology (AEPC), International Society for Heart and Lung Transplantation (ISHLT). Eur Heart J 2016;37:67-119.
29. Ishida Y, Yoshinaga K, Miyagawa M, Moroi M, Kondoh C, Kiso K, et al.

Recommendations for (18)F-fluorodeoxyglucose positron emission tomography imaging for cardiac sarcoidosis: Japanese Society of Nuclear Cardiology recommendations. Ann Nucl Med 2014;28:393-403.

30. Pencina MJ, D'Agostino RB, Sr., D'Agostino RB, Jr., Vasan RS. Evaluating the added predictive ability of a new marker: from area under the ROC curve to reclassification and beyond. Stat Med 2008;27:157-72.

31.Dobarro D, Schreiber BE, Handler C, Beynon H, Denton CP, Coghlan JG. Clinical characteristics, haemodynamics and treatment of pulmonary hypertension in sarcoidosis in a single centre, and meta-analysis of the published data. Am J Cardiol 2013;111:278-85.

32. Murtagh G, Laffin L.J, Patel K.V, Patel AV, Bohnam C.A, Yu Z, et.al. Improved detection of myocardial damage in sarcoidosis using longitudinal strain in patients with preserved left ventricular ejection fraction. Echocardiography2016.33(9):1344-1352

33. Kandolin R, Lehtonen J, Airaksinen J, Vihinen T, Miettinen H, Ylitalo K, Kaikkonen K, Tuohinen S, Haataja P, Kerola T, Kokkonen J. Cardiac sarcoidosis: epidemiology, characteristics, and outcome over 25 years in a nationwide study. Circulation. 2015 ;624-32.

13- Acknowledgments

I would like to express my thanks and gratitude to Professor Masaki Ieda for giving me this chance to do research and training in the cardiology department and for his support. My appreciation and thanks to the inspiring teacher, Dr. Tomoko Ishizu, for her supervision and support. Special thanks and gratefulness to Dr. Kimi Sato for her advice, effort, and time in mentoring my research through the Ph.D. program. My thanks to all cardiology staff that I learned from them directly or indirectly. All thanks to cardiology sonographers, whom I learned a lot, and for being friendly and encouraging, especially (Dr. Norika Iida, Dr. Hideki Nakajima, and Mr. Hiroyuki Naito), who let me enjoy learning and enlighten my journey.

My deep thanks and respect to the kind-heart patients in Tsukuba University Hospital; without them, I couldn't learn and do research.

Finally, I would like to acknowledge my thanks to my loving family, my parents, siblings, my husband (Qasim), and my daughter (Zahraa) for their continuous support and love that keep me going and cheer my life.

14.Tables

Table 1. Patient characteristics at baseline according to events.

	Entire cohort n=51	Event n=11 (22%)	No event n=40 (78%)	*p*-value
Age, years	63±11	65±9	63±11	0.45
Sex, female, n (%)	31 (61)	7 (64)	24 (60)	0.83
Body surface area, m^2	1.60±0.20	1.60±0.20	1.60±0.21	0.93
NYHA functional class III/IV, n (%)	3 (6)	1 (9)	2 (5)	0.61
Diabetes mellitus, n (%)	6 (12)	0	6 (15)	0.17
Chronic lung disease, n (%)	5 (10)	1 (9)	4 (10)	0.93
Heart failure, n (%)	5 (10)	2 (18)	3 (8)	0.29
Beta-blocker use, n (%)	26 (51)	5 (46)	21 (53)	0.68
ACEI/ARB use, n (%)	27 (53)	6 (55)	21 (53)	0.90
mineralocorticoid receptor antagonists, n (%)	11 (22)	3 (27)	8 (20)	0.603
Furosemide, n (%)	5 (13)	0	5	0.211
Amiodarone, n (%)	15 (29)	6 (55)	9 (23)	0.039
Implanted cardiac device, n (%)				0.534
Pacemaker, n (%)	11 (22)	3 (27)	8 (20)	
ICD, n (%)	5 (10)	2 (18)	3 (8)	
CRTD, n (%)	3 (6)	0	3 (8)	
Creatinine, mg/dL	0.84±0.28	0.80±0.21	0.85±0.30	0.59
BNP level, pg/mL	154 (62–293)	109 (92–212)	174 (56–327)	0.36
ACE elevation (> 29.4 IU/L), n (%)	6 (12)	0	6 (15)	0.17
sIL-2R elevation (> 613 U/ml), n (%)	14 (28)	2 (18)	12 (30)	0.44
Extracardiac sarcoidosis, n (%)	32 (63)	5 (46)	27 (68)	0.18
Eye, n (%)	8 (16)	2 (18)	6 (15)	0.80
Lung, n (%)	26 (51)	3 (27)	23 (58)	0.08
Skin, n (%)	3 (6)	1 (9)	2 (5)	0.61
Arrhythmic event, n (%)	30 (59)	9 (89)	21 (53)	0.08
FDG-PET abnormality, n (%)	50 (98)	10 (91)	40 (100)	0.054

LGE on CMR, n (%)	33 (97)	5 (46)	26 (65)	0.24

ACE, angiotensin-converting enzyme; ACEI, angiotensin-converting enzyme inhibitor; ARB, angiotensin II receptor blocker; BNP, brain natriuretic peptide; FDG-PET, fluorodeoxyglucose positron emission tomography; LGE, late gadolinium enhancement; NYHA, New York Heart Association; RV, right ventricle; RVD, right ventricular dysfunction; sIL-2R, soluble interleukin-2 receptor; CMR, cardiac magnetic resonance imaging.

Table 2. Criteria for Cardiac Involvement According to JCS Guidelines

	All N = 51	Event n=11 (22%)	No event n=40 (78%)	*p*-value
1. Major criteria				
(a) High-grade atrioventricular block or fatal ventricular arrhythmia				
High-grade atrioventricular block, n (%)	20 (39)	6 (55)	14 (35)	0.24
Ventricular tachycardia, n (%)	15 (30)	7 (64)	8 (20)	0.005
Ventricular fibrillation, n (%)	2 (4)	0	2 (5)	0.449
(b) Basal thinning of the ventricular septum or abnormal ventricular wall anatomy (aneurysm, thinning, thickening of ventricular wall)				
Basal thinning of the ventricular septum, n (%)	21 (41)	7 (64)	14 (35)	0.09
Abnormal ventricular wall anatomy, n (%)	12 (24)	2 (18)	10 (26)	0.609
(c) Left ventricular ejection fraction < 50% or regional wall motion abnormality				
Left ventricular ejection fraction < 50%, n (%)	25 (49)	5 (46)	20 (50)	0.789
Regional wall motion abnormality, n (%)	39 (77)	9 (82)	30 (75)	0.64
(d) Abnormal cardiac accumulation on ^{67}Ga citrate scintigraphy of FDG-PET, n (%)	50 (98)	10 (91)	40 (100)	0.054
(e) Late gadolinium enhancement on CMR, n (%)	34 (97)	5 (46)	26 (65)	0.24
2. Minor criteria				
(f) Abnormal ECG findings: ventricular arrhythmias (nonsustained VT, multifocal or frequent PVC), bundle branch block, axis deviation, or abnormal Q waves, n (%)	30 (67)	6 (55)	24 (71)	0.327
(g) Perfusion defects on myocardial perfusion scintigraphy (SPECT), n (%)	0 (0)	0 (0)	0 (0)	NA
(h) Endomyocardial biopsy: monocyte infiltration and moderate or severe myocardial interstitial fibrosis, n (%)	25 (49)	6 (55)	19 (48)	0.68

Abbreviations: CMR, cardiac magnetic resonance imaging; ECG, electrocardiogram; JCS, Japanese circulation society; FDG-PET, 18F-fluorodeoxyglucose positron emission

tomography; PVC, premature ventricular contraction; SPECT, single-photon emission computed tomography; VT, ventricular tachycardia.

Table 3. Echocardiographic characteristics at baseline according to events.

	Entire cohort n=51	Event n=11 (22%)	No event n=40 (78%)	*p*-value
LVEDVi, mL/m²	78±34	72±24	80±36	0.47
LVESVi, mL/m²	34.5 (24–53)	32 (27–46)	35 (24–54)	0.87
LVEF, %	50±14	47±12	50±14	0.49
Basal IVS thinning, n (%)	21 (41)	7 (64)	14 (35)	0.09
Aneurysm, n (%)	12 (24)	2 (18)	10 (25)	0.64
Regional wall motion abnormality, n (%)	39 (77)	9 (82)	30 (75)	0.64
LVEF <50% n (%)	25 (49)	5 (46)	20 (50)	0.79
LVMi, g/m²	115±33	122±36	114±32	0.48
E/A	0.84 (0.71–1.16)	0.92 (0.71–1.57)	0.83 (0.71–1.13)	0.62
E/e'	10.4 (7.5–13.6)	9.8 (6.8–13.3)	10.6 (7.5–14.3)	0.66
LAVi, mL/m²	38±15	36±13	39±16	0.67
LV GLS, %	-12.3±4.5	-12.0±3.6	-12.3±4.8	0.85
MR ≥ moderate, n (%)	18 (35)	1 (9)	17 (43)	**0.04**
TR ≥ moderate, n (%)	6 (12)	2 (18)	4 (10)	0.46
TR velocity, m/sec	2.24 (1.94-2.43)	2.24 (2.04-2.38)	2.25 (1.93-2.44)	0.98
TAPSE, mm	21±4	20.5±5.4	20.8±3.5	0.84
S', cm/s	11.5±2.3	10.9±2.5	11.6±2.3	0.47
FAC, %	36±10	34±11	37±9	0.45
RVFWLS, %	-19.1±5.2	-15.7±4.0	-20.1±5.1	**0.013**

IVS, interventricular septum; FAC, fractional area change; GLS, global longitudinal strain; LAVi, left atrial volume index; LV, left ventricular; LVEDVi, left ventricular end-diastolic volume index; LVEF, left ventricular ejection fraction; LVESVi, left ventricular end-systolic volume index; LVMi, left ventricular mass index; MR, mitral regurgitation; RVD, right ventricular dysfunction; RVFWLS, right ventricular free wall longitudinal strain; S', tricuspid lateral annular systolic velocity on tissue Doppler imaging; TAPSE, tricuspid annular plane systolic excursion; TR, tricuspid regurgitation.

Table 4. Treatment after diagnosis

	Entire cohort n=51	**Event n=11 (22%)**	**No event n=40 (78%)**	***p*-value**
Steroid maintenance dose, mg				0.074
Steroid dose ≤ 5 mg, n (%)	23 (48)	6 (60)	17 (45)	
Steroid dose > 5 - 10 mg, n (%)	24 (50)	3 (30)	21 (55)	
Steroid dose >10 mg, n (%)	1 (2)	1(9)	0	
Implanted cardiac device, n (%)				0.555
Pacemaker, n (%)	6 (12)	1 (9)	5 (13)	
ICD, n (%)	5 (10)	1 (9)	4 (10)	
CRTD, n (%)	7 (14)	3 (27)	4 (10)	
Methotrexate, n (%)	7 (14)	3 (27)	4 (10)	0.140
Azathioprine, n (%)	1 (2)	0	1 (3)	0.592

ICD, Implantable cardioverter defibrillator; CRTD cardiac resynchronization therapy (CRTD).

Table 5. Cox proportional hazards model for composite endpoints of cardiovascular events.

	Univariable		Multivariable	
	HR (95% CI)	p-value	HR (95% CI)	p-value
Age, years	1.04 (0.97–1.11)	0.26		
Female sex	1.18 (0.34–4.04)	0.80		
Atrioventricular block at baseline	1.53 (0.46-5.11)	0.49		
Sustained VT at baseline	5.26 (1.54-18.05)	0.008	4.20 (1.16-15.17)	0.028
LVEF, %	0.97 (0.93–1.02)	0.25		
LV GLS, %	1.03 (0.89-1.18)	0.72		
TR velocity, m/sec	1.78 (0.54–5.80)	0.34		
TAPSE, mm	0.96 (0.82–1.14)	0.67		
S', cm/s	0.89 (0.65–1.22)	0.47		
FAC, %	0.97 (0.92–1.03)	0.37		
RVFWLS, %	1.29 (1.07–1.57)	0.008	1.22 (1.03–1.46)	0.025

CI, confidence interval; FAC, fractional area change; GLS, global longitudinal strain; HR, hazard ratio; LV, left ventricular; LVEF, left ventricular ejection fraction; RVFWLS, right ventricular free wall longitudinal strain; S', tricuspid lateral annular systolic velocity on tissue Doppler imaging; TAPSE, tricuspid annular plane systolic excursion; TR, tricuspid regurgitation; VT, ventricular tachycardia.

Table 6. Paired comparison for RV conventional and RVFWLS parameters according to the RV systolic function at the baseline and 1-year follow-up.

	Event			No event			*p*-value†
	Baseline	**Follow-up**	***p*-value***	**Baseline**	**Follow-up**	***p*-value***	
TAPSE, mm	20.5±5.4	17.7±3.6	0.06	20.8±3.5	20.5±4.0	0.43	0.07
S', cm/s	11.0±2.5	10.3±1.8	0.65	11.6±2.3	11.0±1.6	0.16	0.28
FAC, %	33.9±11.3	33.3±10.6	0.79	36.6±9.4	37.6±9.6	0.44	0.39
RVFWLS, %	-15.7±4.0	-14.5±2.6	0.09	-20.1±5.1	-20.8±5.4	0.56	**0.002**
LVEF, %	47.2±12.1	50.3±10.8	0.11	50.2±14.2	53.3±13.9	0.40	0.56
LV GLS, %	-12.0±3.6	-10.5±2.8	0.13	-12.3±4.8	-14.5±4.3	**0.004**	**0.014**

*Comparison between baseline and follow-up in the same group performed using paired test.

†Comparison between follow-up in the event and event-free groups performed using unpaired test.

FAC, fractional area change; GLS, global longitudinal strain; LV, left ventricular; LVEF, left ventricular ejection fraction; RV, right ventricular; RVFWLS, right ventricular free wall longitudinal strain; S', tricuspid lateral annular systolic velocity on tissue Doppler imaging; TAPSE, tricuspid annular plane systolic excursion.

Table 7. Patients' characteristics according to the RVFWLS

	Reduced RVFWLS: >-16.8% N = 18 (35%)	Preserved RVFWLS: ≤-16.8% N = 33 (65%)	**p-value**
BNP, pg/mL	223 (109-437)	113 (51-201)	**0.032**
LVEDVi, mL/m^2	84±42	75±29	0.40
LVESVi, mL/m^2	38 (27-80)	31 (21-47)	0.10
LVEF, %	42.4±11.9	53.4±13.3	**0.005**
LV GLS, %	-10.4±3.9	-13.3±4.6	**0.049**
TR velocity, m/sec	2.31 (2.03-2.84)	2.22 (1.90-2.42)	0.18

BNP, brain natriuretic peptide; GLS, global longitudinal strain; LAVi, left atrial volume index; LV, left ventricular; LVEDVi, left ventricular end-diastolic volume index; LVEF, left ventricular ejection fraction; LVESVi, RVFWLS, right ventricular free wall longitudinal strain; TR, tricuspid regurgitation.

Table 8. Association between RV uptake on ^{18}F-fluorodeoxyglucose positron emission tomography and echocardiographic parameters.

	FDG-PET		
	RV uptake (+) n=19 (38%)	**RV uptake (-) n=26 (62%)**	**P-value**
LVEF, %	51±11	48±15	0.59
LV GLS, %	-12.2±3.6	-12.3±5.0	0.91
TAPSE, mm	20±5	21±3	0.49
S', cm/s	11.2±2.8	11.7±2.1	0.53
FAC, %	30.0±10.0	39.3±8.1	0.001
RVD by conventional parameters, n (%)	5 (56)	14 (34)	0.27
RVFWLS, %	-17.0±3.9	-20.6±5.5	0.018

FAC, fractional area change; GLS, global longitudinal strain; LV, left ventricular LVEF, left ventricular ejection fraction; RV, right ventricular; RVD, right ventricular dysfunction; RVFWLS, right ventricular free wall longitudinal strain; S', tricuspid lateral annular systolic velocity on tissue Doppler imaging; TAPSE, tricuspid annular plane systolic excursion.

Table 9. Association between RV Late gadolinium enhancement on cardiac magnetic resonance imaging and echocardiographic parameters.

	CMR		
	RV LGE (+) n=15 (44%)	**RV LGE (-) n=19 (65%)**	**P-value**
LVEF, %	49±10	52±16	0.49
LV GLS, %	12±3	13±5	0.35
TAPSE, mm	20±5	21±3	0.64
S', cm/s	12±3	12±2	0.89
FAC, %	32±10	39±8	0.046
RVD by conventional parameters, n (%)	4 (27%)	1 (5%)	0.08
RVFWLS, %	16.6±4	20.5±5	0.022

FAC, fractional area change; GLS, global longitudinal strain; LV, left ventricular; LVEF, left ventricular ejection fraction; RV, right ventricular; RVD, right ventricular dysfunction; RVFWLS, right ventricular free wall longitudinal strain; S', tricuspid lateral annular systolic velocity on tissue Doppler imaging; TAPSE, tricuspid annular plane systolic excursion.

Table 10. LGE distribution and FDG accumulation according to the baseline RVFWLS (N = 33).

	Reduced RVFWLS: >-16.8% N= 13 (39%)	**Preserved RVFWLS: ≤-16.8% N=20 (61%)**	**P value**
CMR data			
LGE mass in LV, g	31 ± 16	26 ± 24.6	0.558
Segmental LGE distribution			
Basal septum, n (%)	12 (92)	16 (80)	0.335
Mid septum, n (%)	11 (85)	11 (55)	0.078
LV anterior wall, n (%)	9 (69)	8 (40)	0.101
LV anterolateral wall, n (%)	7 (54)	12 (60)	0.727
LV inferolateral wall, n (%)	5 (39)	8 (62)	0.93
LV Inferior wall, n (%)	8 (62)	12 (60)	0.930
LV apex, n (%)	3 (23)	5 (25)	0.900
RV free wall, n (%)	10 (83)	5 (25)	0.001
RV septum, (%)	11 (85)	10 (50)	0.043
FDG-PET data			
Regional uptake			
Basal septum, n (%)	9 (69)	15 (75)	0.716
Mid septum, n (%)	11 (85)	13 (65)	0.216
LV anterior wall, n (%)	7 (54)	6 (30)	0.171
LV anterolateral wall, n (%)	8 (62)	16 (80)	0.245
LV inferolateral wall, n (%)	8 (62)	14 (70)	0.614
LV Inferior wall, n (%)	7 (54)	9 (45)	0.619
LV apex, n (%)	7 (54)	10 (50)	0.829
RV free wall, n (%)	8 (62)	7 (35)	0.135

CMR, cardiac magnetic resonance imaging; 18F-fluorodeoxyglucose positron emission tomography; LGE, late gadolinium enhancement; left ventricular, LV; RV, right ventricular; RVFWLS, right ventricular free wall longitudinal strain

Table 11. Catheter ablation details

Patients no.	Age (years)	Gender	LVEF (%)	RVFWLS (%)	Low voltage area	Ablation site
1	65	male	48	-20.0	LV septum RV septum	LV septum RV septum
2	59	male	49	-17.0	RV septum	RV septum
3	68	female	56	-15.7	Normal voltage	LV anterolateral wall
4	54	female	35	-16.0	LV septum RV septum	LV septum RV septum LVOT RVOT
5	75	male	43	-21.7	Normal voltage	RV septum
6	82	male	51	-11.8	RV free wall	LV anterior wall
7	69	female	30	-12.0	RV septum	LVOT RVOT

LV left ventricular; LVEF, left ventricular ejection fraction; LVOT, left ventricular outflow tract, RV, right ventricular; RVFWLS, right ventricular free wall longitudinal strain, RVOT; right ventricular outflow tract.

15- Figures

Figure1. Histopathological findings of cardiac sarcoidosis.

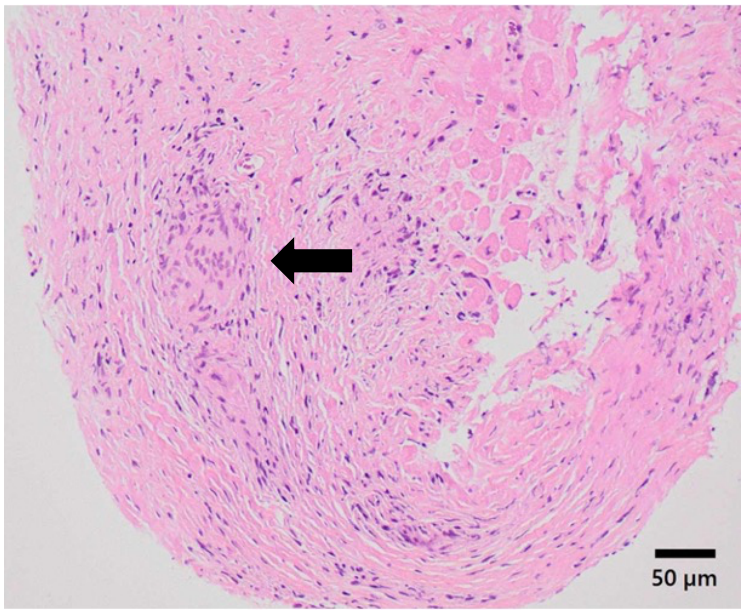

Representative image of endomyocardial biopsy specimen in a study population (hematoxylin and eosin stain). The myocardial specimen obtained from right ventricular septum showed non-caseating epithelioid cell granulomas (arrow).

Figure 2. Echocardiographic parameters for right ventricular function assessment

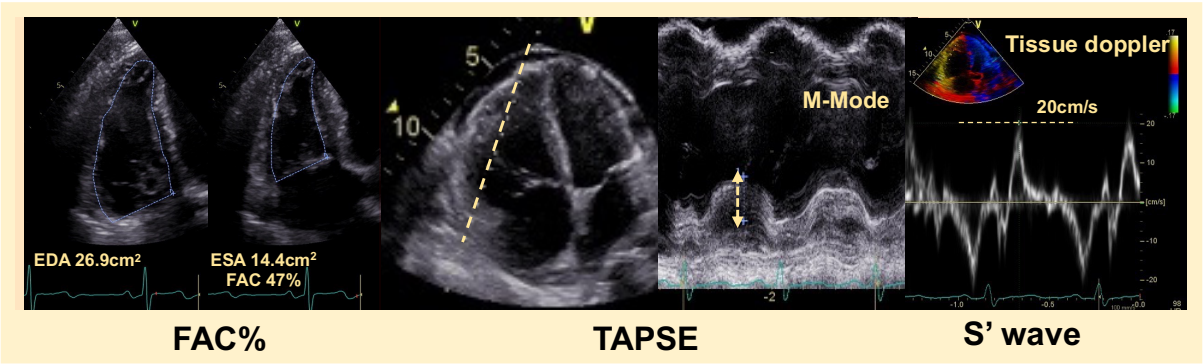

This figure shows echocardiographic parameters for the right ventricular function assessment parameters: Fractional area change (FAC), Tricuspid annular plane systolic excretion (TAPSE), Tricuspid lateral annular systolic velocity (S').

Figure 3. Right ventricular free wall longitudinal strain (RVFWLS)

(A) Schematic figure for the strain analysis

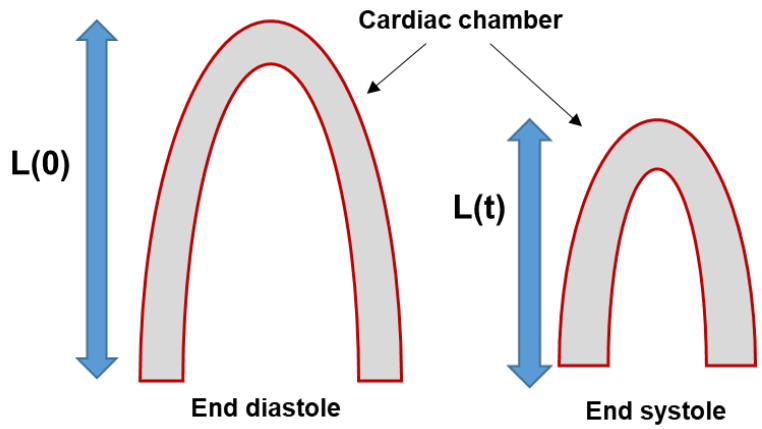

$$Strain = \frac{L(t) - L0}{L0}$$

The strain can be evaluated as the change of the length in one direction from the reference time (L0) to a given point in time (L(t)) and described as a percent. The reference time is usually taken at end-diastole and the length in systole is less than the length in diastole so the value of strain would be negative number if their myocardial function is normal.

(B) Preserved RVFWLS

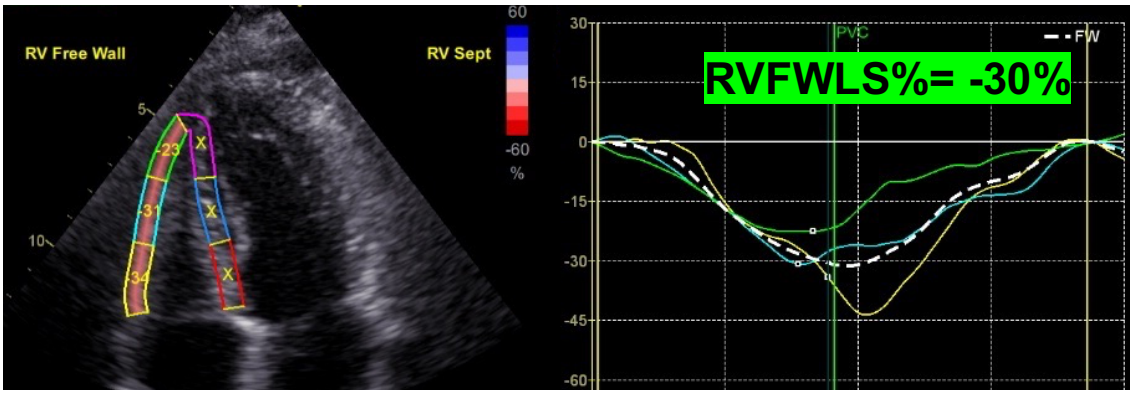

(C) Reduced RVFWLS

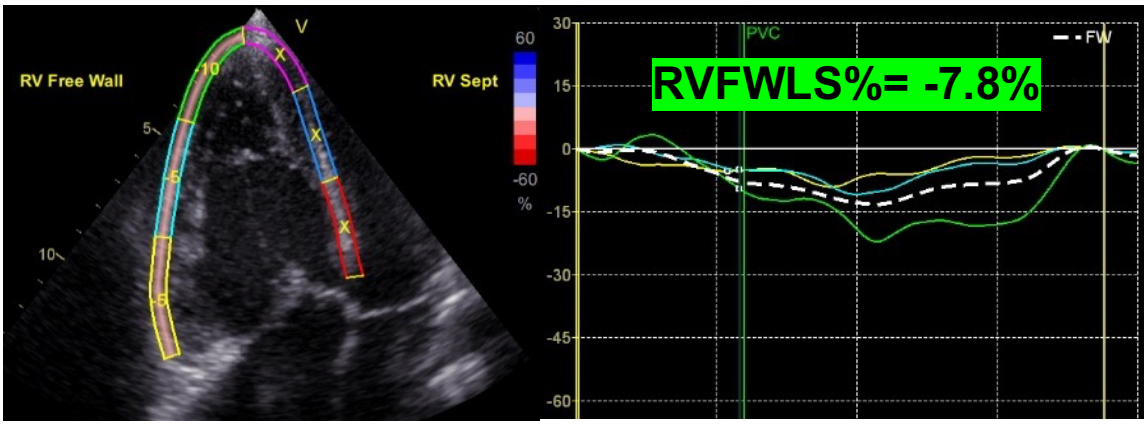

The larger absolute number of the strain means better longitudinal ventricular function, while lower absolute number of the strain means deteriorated ventricular function. Patients with RVFWLS = -30% (B), the absolute number is 30 which indicated good RV function, while a patient with RVFWLS = - 7.8 % (C), the absolute number is 7.8, indicating RV dysfunction.

Figure 4. Study flow diagram

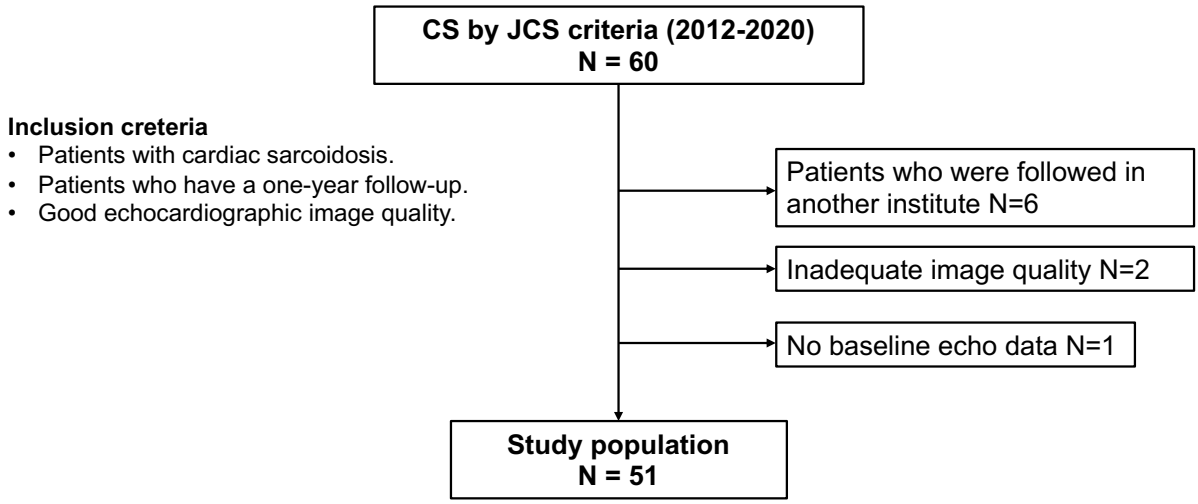

Figure 5. Speckle tracking imaging, 18F-fluorodeoxyglucose positron emission tomography, and cardiac magnetic resonance imaging evaluation of right ventricle.

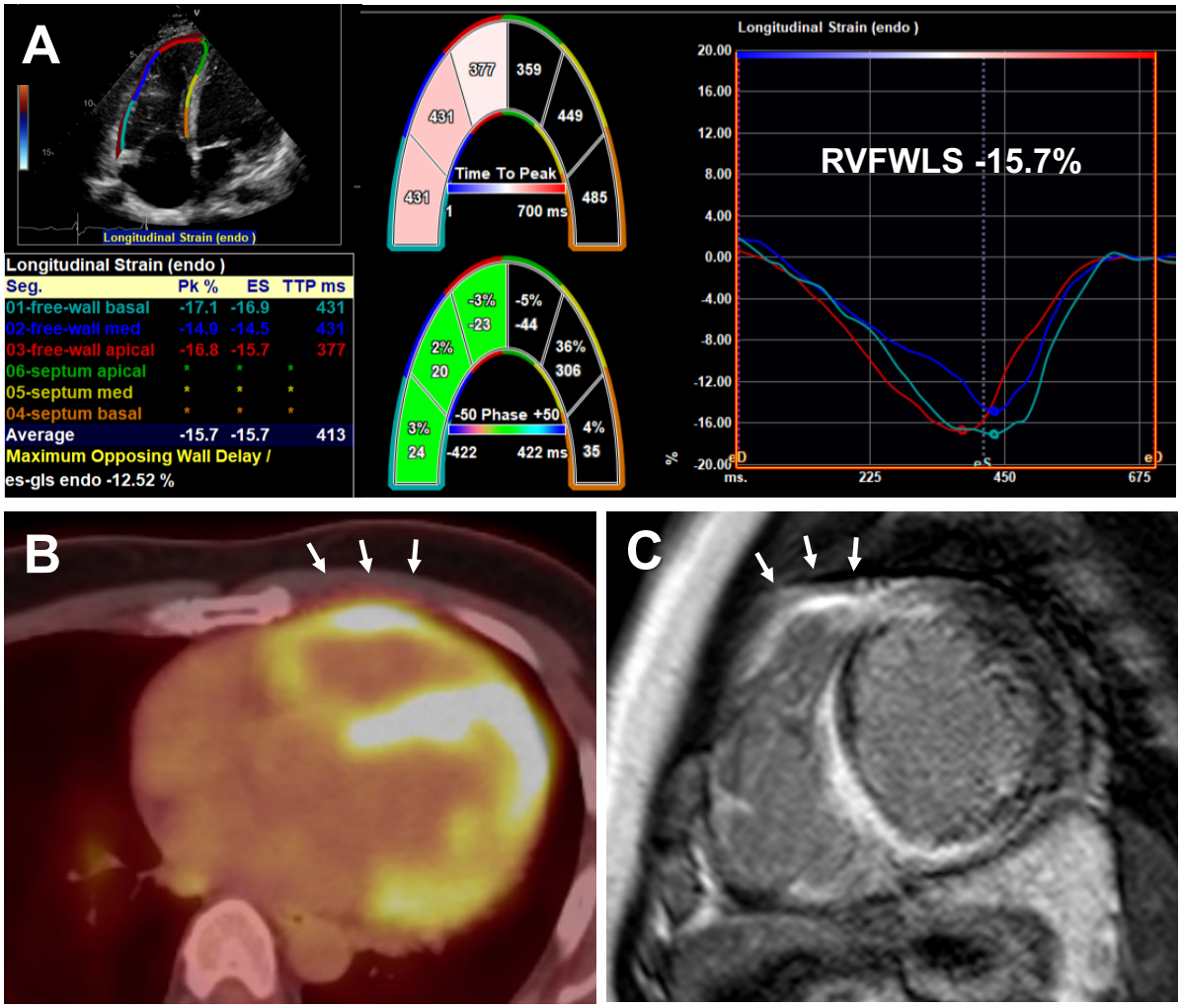

The figure shows right ventricular free wall longitudinal strain (RVFWLS; A), ^{18}F-fluorodeoxyglucose on fluorodeoxyglucose positron emission tomography evaluation (FDG-PET; B), and cardiac magnetic resonance imaging (CMR; C) in cardiac sarcoidosis patient. RVFWLS was estimated by assessing the average longitudinal strain in the RV free wall segment after excluding the septal component. RVFWLS was estimated to be -15.7 %, indicating deterioration of RV longitudinal systolic function. FDG-PET showed intense uptake in the RV free wall (arrow). CMR also showed late gadolinium enhancement in the RV free wall (arrow).

Figure 6. Segmental evaluation of RV and LV involvement.

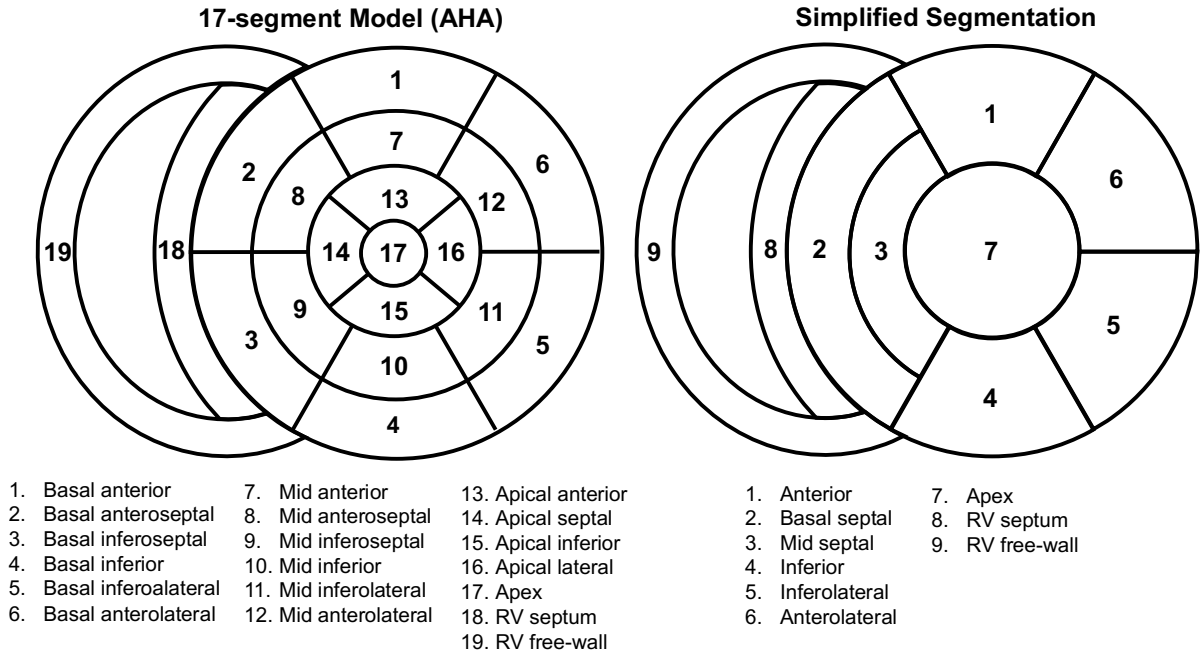

LV myocardial segmentation was performed using the American Heart Association 17-segment model [27]. For analysis, we simplified the LV segmentation; for septal segments, anteroseptal and inferoseptal segments in basal and mid were considered the same segment. As for remaining anterior, anterolateral, inferolateral, and inferior segments, basal and mid segments were merged and considered as the same segment. Four apical segments and an apex were exhibited as one segment. The endocardial RV surface was divided into RV-free wall and septum.

Figure 7. Flow diagram of diagnosis of cardiac sarcoidosis according to JCS guidelines

Abbreviations: CS, cardiac sarcoidosis; JCS, Japanese circulation society

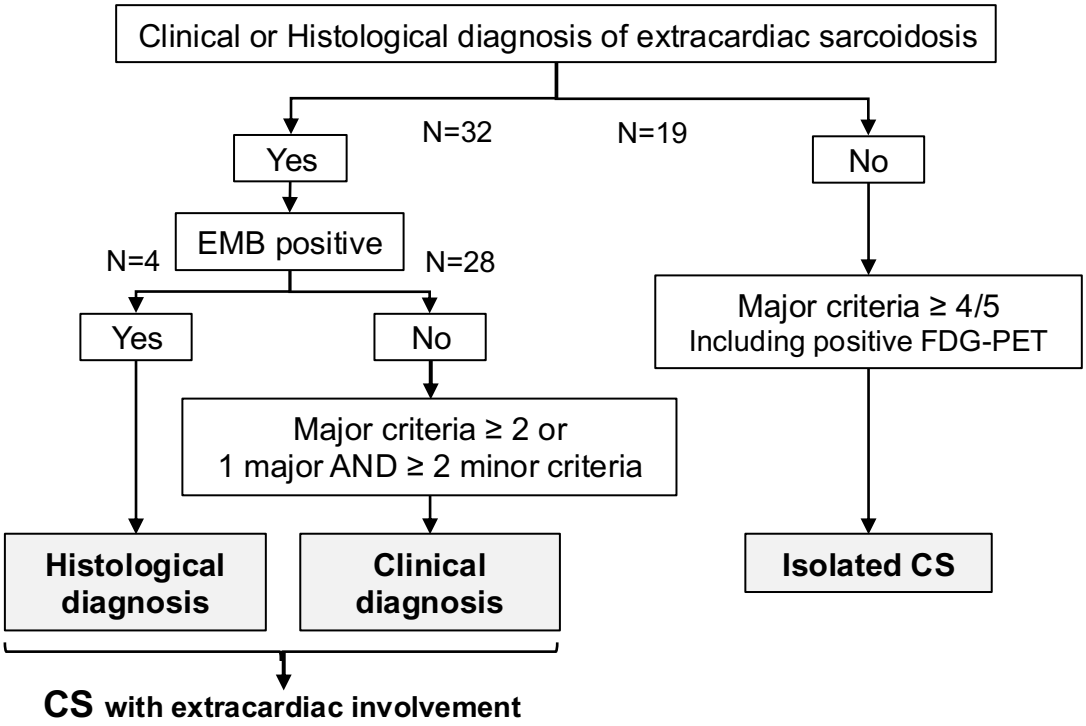

Major Criteria
• Heart block, fatal ventricular arrhythmia • Basal IVS thinning, abnormal wall anatomy • LVEF < 50% or wall motion abnormality • Cardiac uptake in FDG-PET or Ga scintigraphy • LGE on CMR
Minor Criteria
• Abnormal ECG findings: ventricular arrythmia, bundle branch block, axis deviation, abnormal Q wave • Perfusion defect on SPECT • Interstitial fibrosis or monocyte infiltration on EMB

Figure 8. Impact of baseline RVFWLS on outcomes in patients with cardiac sarcoidosis.

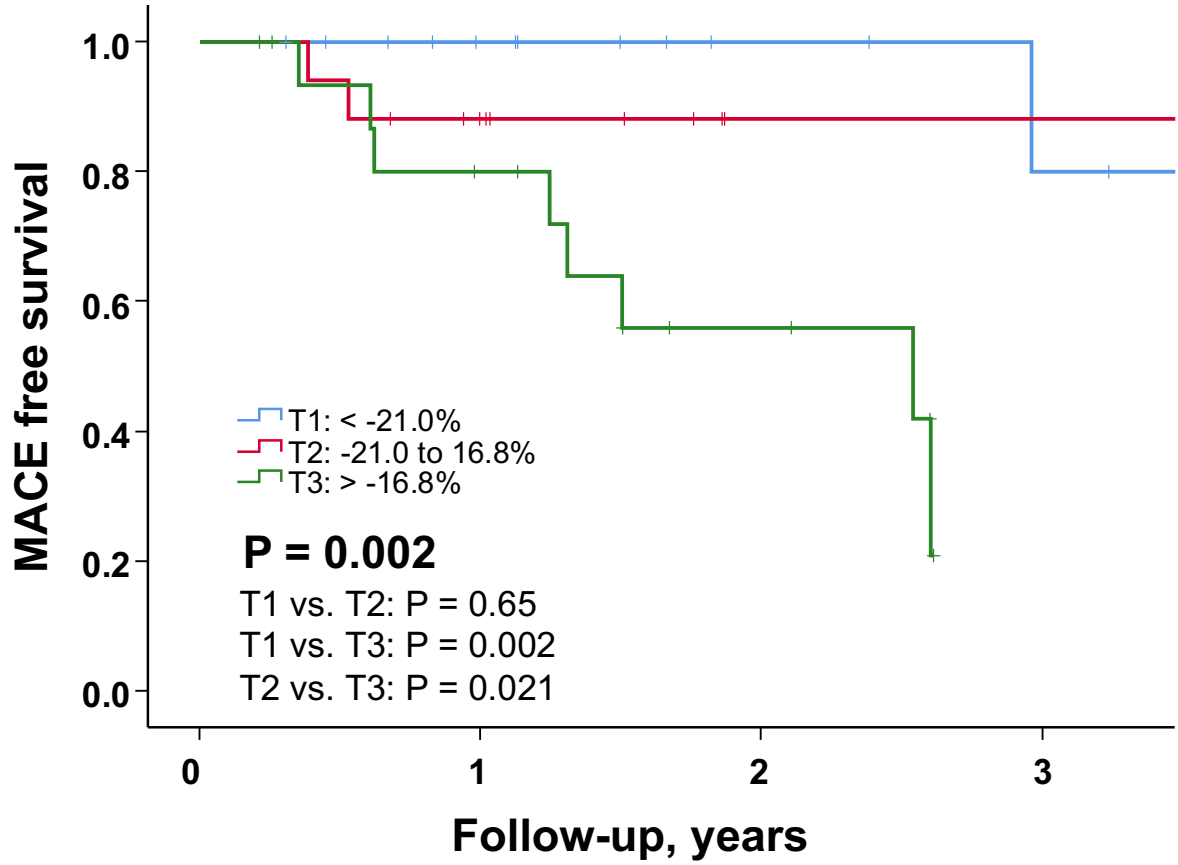

Pts. at risk	0	1	2	3
T1	17	11	6	4
T2	17	12	6	6
T3	17	11	5	0

Kaplan-Meier curves demonstrated MACE-free survival in patients with cardiac sarcoidosis according to the RVFWLS tertiles. Patients with RVFWLS >-16.8% (third tertile) had lower MACE-free survival than those in the other groups (p=0.002).

MACE, major adverse cardiovascular event; RVFWLS, right ventricular free wall longitudinal strain; T, tertile.

Figure 9. Receiver-operating characteristic curves to detect patients with major adverse cardiovascular events.

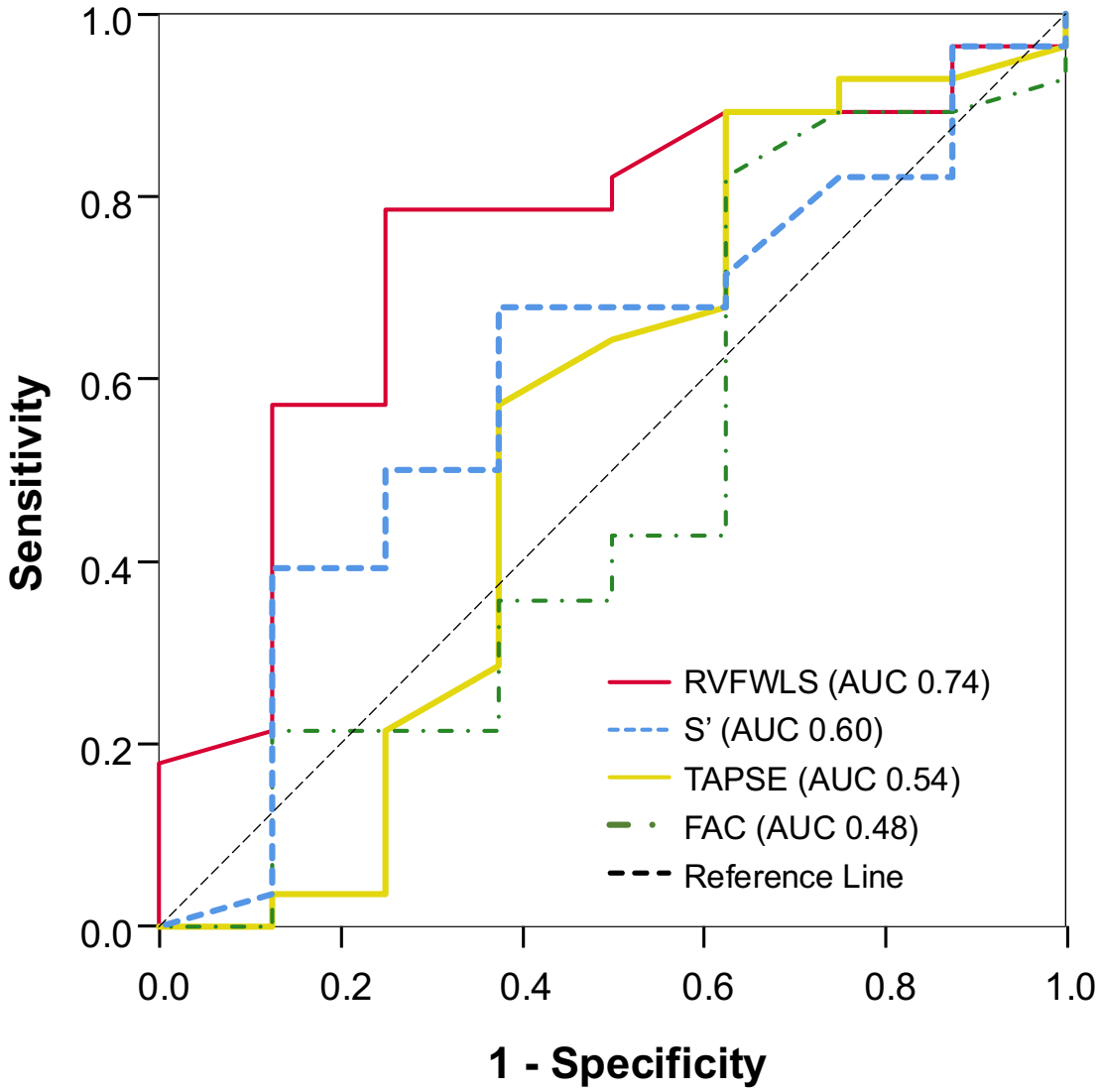

Baseline right ventricular free wall longitudinal strain (RVFWLS) showed the highest area under the curve (AUC: 0.74) among echocardiographic markers of right ventricular function at the baseline to detect major adverse cardiovascular events.

FAC, fractional area change; TAPSE, tricuspid annular plane systolic excretion.

Figure 10. Changes in echocardiographic parameters during steroid therapy in cardiac sarcoidosis patients with and without events.

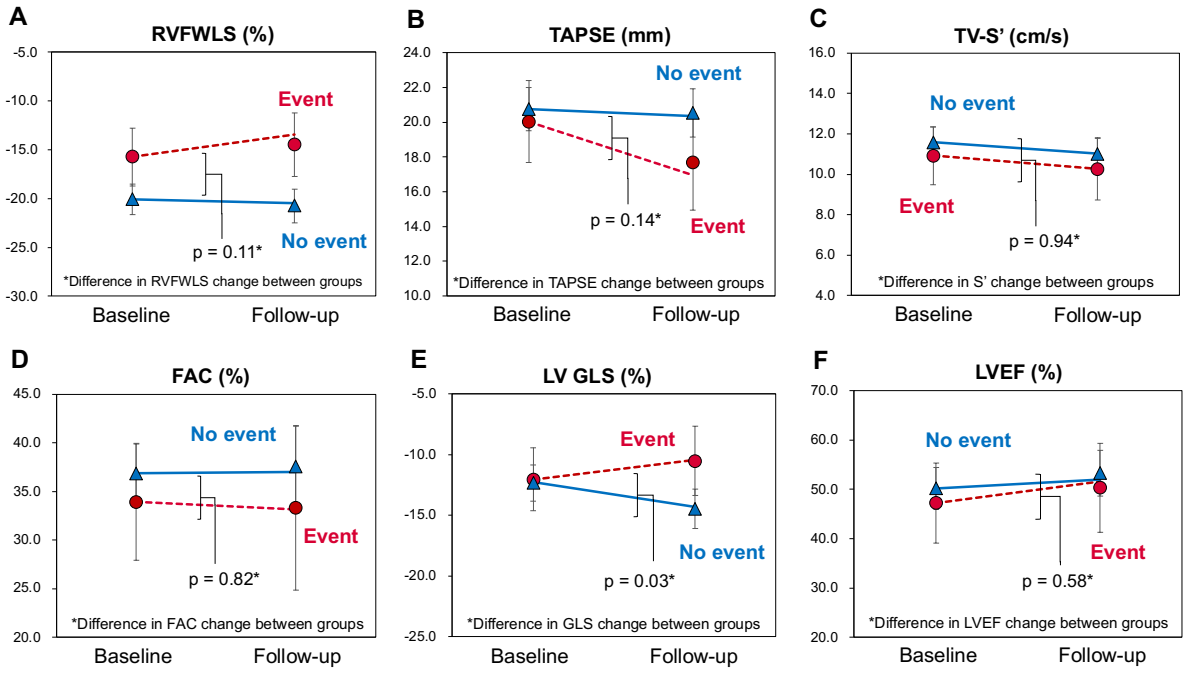

Markers represent the average of the observed data obtained at baseline and 1 year after steroid therapy. Error bars represent 95% confidence intervals. The regression line was obtained by the mixed-model approach. The model was constructed with the patients' group, change over time, and interaction between groups and change (showing if magnitude of changes is different between groups). RVFWLS showed trend towards worsening in patients with events compared with the no event group (p = 0.11; A). LVGLS showed deterioration in patients with events, while it was improved in patients without events (p = 0.03; E). Patients with events also showed trend toward worsening in TAPSE (B) than those without events at 1 year, while S' (C), FAC (D), and LVEF (F) showed similar changes over time.

FAC, fractional area change; LVEF, left ventricular ejection fraction; LVGLS, left ventricular global longitudinal strain; RVFWLS, right ventricular free wall longitudinal strain; TAPSE, tricuspid annular plane systolic excursion.

Figure 11. Comparison of the distribution of cardiac involvement according to the baseline RVFWLS on LGE CMR (A) and FDG-PET (B).

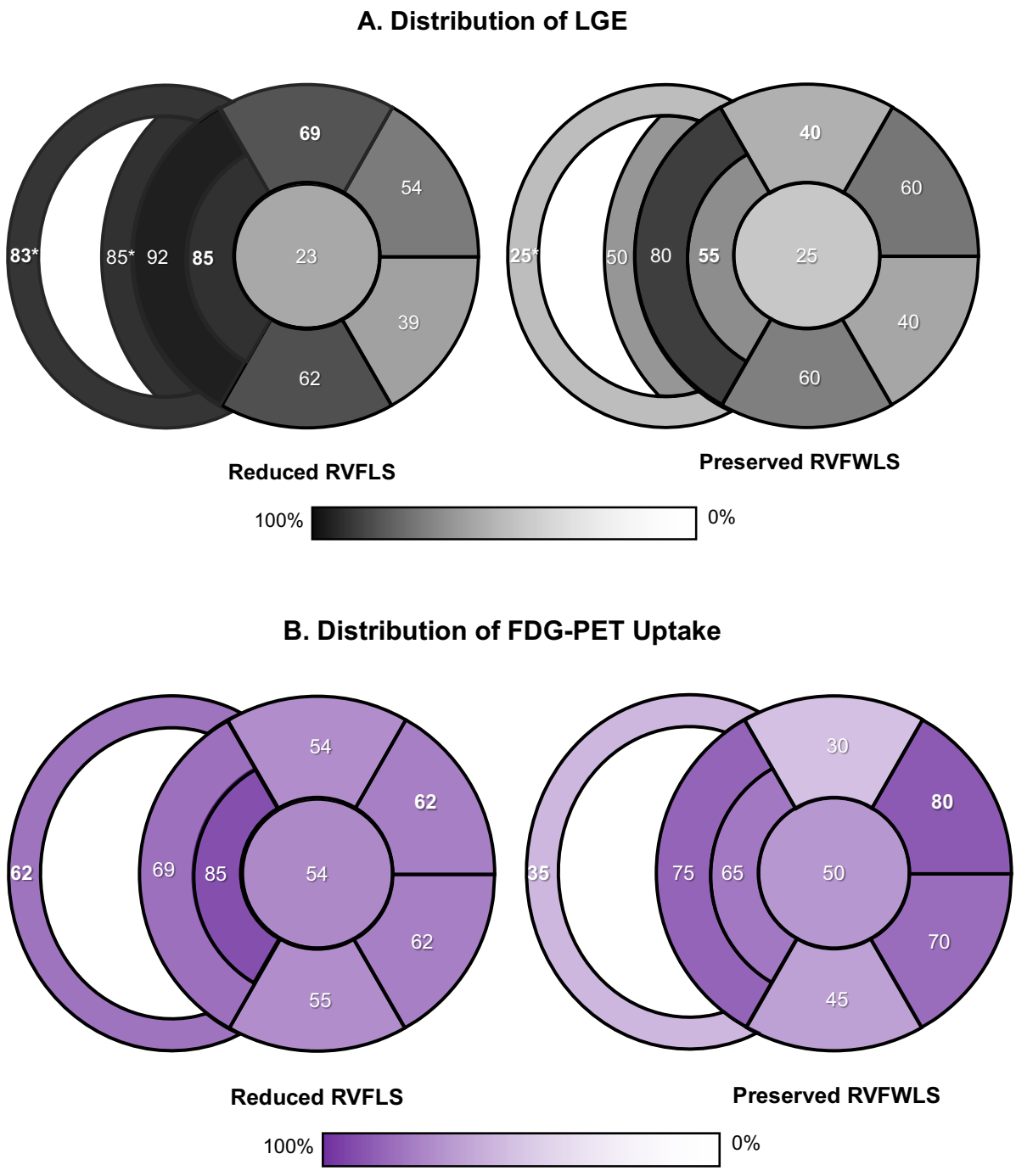

Impaired RVFWLS showed higher prevalence of LGE RV septum, and RV free wall ($p < 0.05$ for all). FDG uptake was not significant between the groups.

Figure 12. Representative cases of LV and RV involvement in CS

(A) Patient with predominant LV involvement

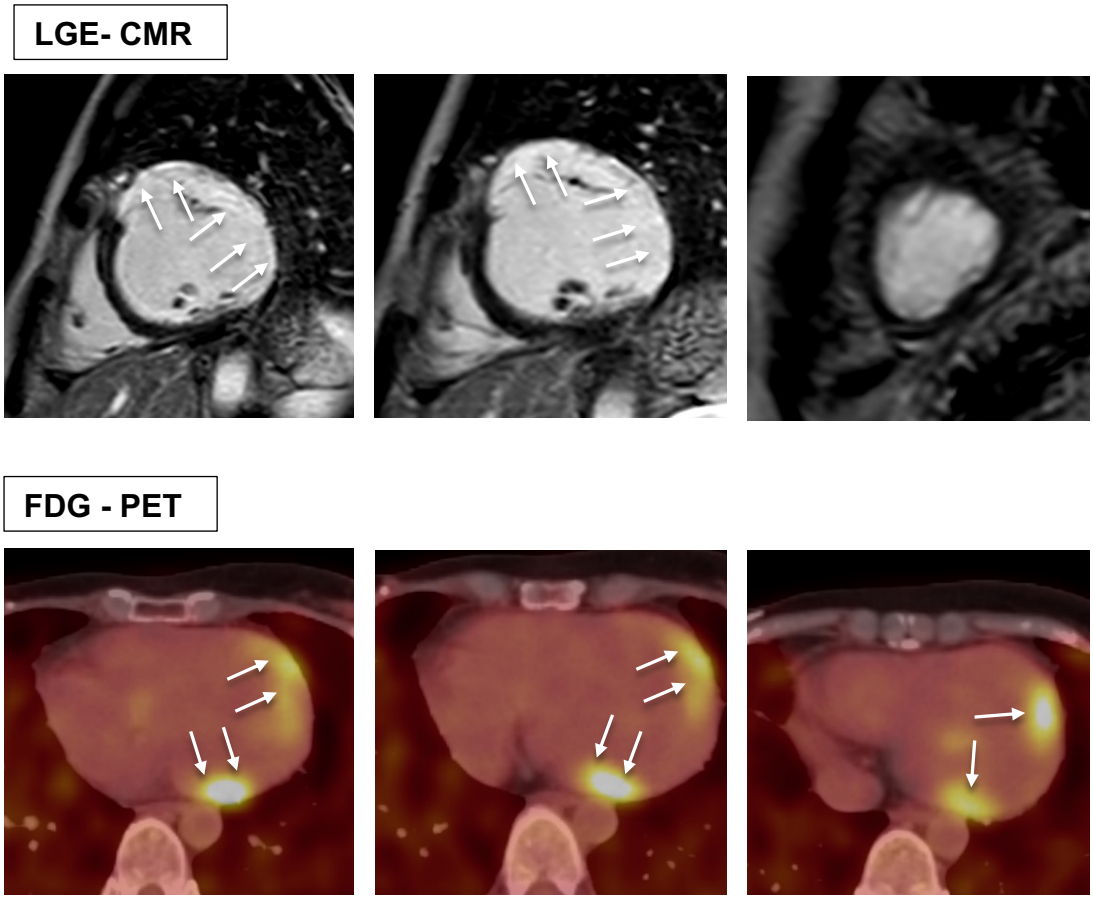

Patient with preserved RV function showed LGE in the LV anterior, lateral, and inferolateral wall (arrow) on CMR. FDG-PET revealed FDG uptake in the LV lateral and inferior wall (arrow).

(B) Patient with predominant RV involvement.

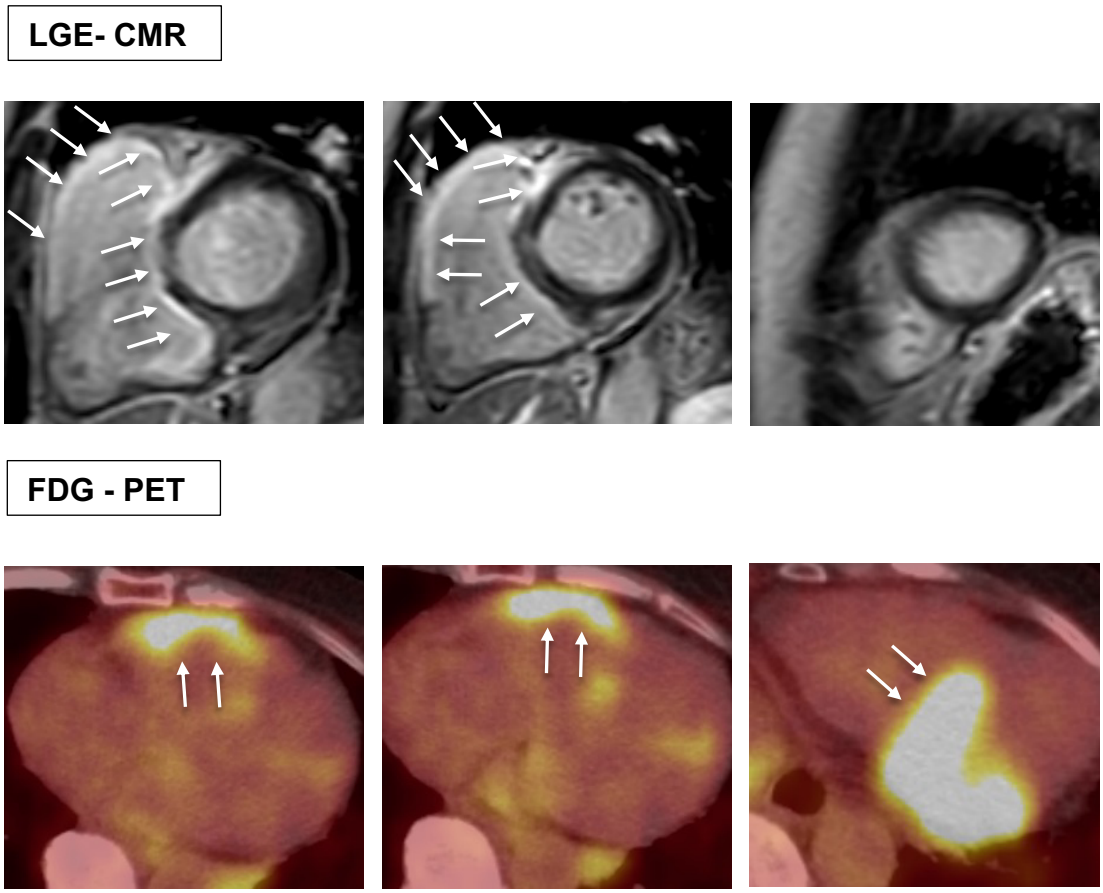

Patient with reduced RV function showed LGE in the RV free-wall and RV septum (arrow) on CMR. FDG-PET showed FDG uptake in the RV free wall (arrow).